UNCLASSIFIED

1

X-822

OAK RIDGE NATIONAL LABORATORY
Operated By
UNION CARBIDE NUCLEAR COMPANY
UCC
POST OFFICE BOX P
OAK RIDGE, TENNESSEE

U.S. ATOMIC ENERGY COMMISSION

External Transmittal
Authorized

ORNL
CENTRAL FILES NUMBER
CF- 57-1-144

COPY NO. 146

DATE: January 31, 1957

SUBJECT: Quarterly Report of the Solution Corrosion Group for the Period Ending January 31, 1957

TO: E. G. Bohlmann

FROM: J. C. Griess, H. C. Savage, J. L. English, R. S. Greeley, S. R. Buxton, D. N. Hess, W. C. Ulrich, T. H. Mauney, and E. F. House

DISTRIBUTION

NOTICE

This document contains information of a preliminary nature and was prepared primarily for internal use at the Oak Ridge National Laboratory. It is subject to revision or correction and therefore does not represent a final report.

~~427 012~~

UNCLASSIFIED

428 001

DISTRIBUTION (Cont'd)

76. E. C. Miller
77. F. C. Moesel, AEC, Wash.
78. G. E. Moore
79. R. L. Moore
80. R. C. Moren
81. C. W. Nestor
82. P. D. Neumann
83. E. O. Nurmi
84. A. R. Olsen
85. L. F. Parsly
86. M. L. Pickelsimer
87. R. M. Pierce
88. L. R. Quarles
89. S. A. Reed
90. D. M. Richardson
91. G. W. Rivenbark
92. R. C. Robertson
93. J. N. Robinson
94. A. M. Rom
95. M. W. Rosenthal
96. H. C. Savage
97. W. F. Schaffer
98. R. E. Schappel
99. H. K. Search
100. C. H. Secoy
101. C. L. Segaser
102. E. H. Shank
103. M. D. Silverman
104. M. J. Skinner
105. I. Spiewak
106. R. W. Stoughton
107. C. D. Susano
108. J. A. Swartout
109. E. H. Taylor
110. D. G. Thomas
111. P. F. Thomason
112. M. Tobias
113. D. S. Toomb
114. W. C. Ulrich
115. W. E. Unger
116. R. Van Winkle
117. R. E. Wacker
118. F. J. Walter
119. R. M. Warner
120. K. S. Warren
121. B. S. Weaver
122. A. M. Weinberg
123. S. H. Wheeler
124. R. R. Wiethaup
125. J. C. Wilson
126. R. H. Winget
127. C. E. Winters
128. L. F. Woo
129. W. C. Yee
130. F. C. Zapp
131. ORNL Document Reference Library, Y-12
132-133. Central Research Library (2)
134-135. REED Library (2)
136. ORNL-RC Lab Records
137-138. Laboratory Records (2)
139-145. Westinghouse - PAR ([illegible])
146-160. AEC, TISE, Oak Ridge (15) ☞

TABLE OF CONTENTS

I. SUMMARY

A second test of the mockup of the Zircaloy - stainless steel transition joint as used in the HRT reactor vessel has been completed. The joint and bellows have now received 104 thermal cycles and 148 mechanical deflections. The joint and bellows have functioned properly; corrosion damage has been negligible, except for a small area on the bellows which has undergone pitting attack.

Long-term runs with uranyl sulfate solutions of the concentration proposed for use in the HRT, viz. 0.04 $\underline{m}$ UO_2SO_4, 0.02 $\underline{m}$ H_2SO_4 and 0.005 $\underline{m}$ $CuSO_4$, have shown the solution to be stable at 300°C. Critical velocities on stainless steel were: 15 to 20 fps at 200°C; 25 to 35 fps at 250°C; and 35 to 40 fps at 300°C. Substituting heavy water for normal water caused no difference in either corrosion or solution stability.

Experiments in which chromic acid was used to pretreat stainless steel have shown that, under certain conditions, the pretreated film can exist in uranyl sulfate solutions at flow rates in excess of the critical velocity for relatively long periods of time.

The practicability of using titanium inserts in highly turbulent areas of stainless steel loops to minimize corrosion has been demonstrated. One 100-A loop was operated for 9900 hr with titanium inserts in regions which normally suffer heavy corrosion. The titanium was essentially unattacked and the crevice between the stainless steel and the titanium caused little corrosion of either the titanium or the stainless steel.

The corrosiveness of beryllium sulfate solutions containing dissolved uranium trioxide has been determined at 250 and 280°C. The solutions showed no advantage over uranyl sulfate solutions of the same concentration. In fact, at low flow rates, the attack in 200 hr was greater in the beryllium-containing solution. On the other hand, at 250 and 300°C, 0.04 $\underline{m}$ UO_2SO_4 containing equimolal beryllium sulfate showed approximately the same corrosion behavior as 0.04 $\underline{m}$ UO_2SO_4 containing 0.02 $\underline{m}$ H_2SO_4.

Laboratory studies with regard to stress-corrosion cracking have shown that highly stressed type 347 stainless steel will crack in boiling uranyl sulfate solutions containing 25 and 50 ppm chloride ions. At chloride concentrations of 0, 5, 10, 100, and 200 ppm, cracking has not been observed; at the 200 and 500 ppm chloride level, suspected cracking has been observed after a 500 hr exposure. Neither bromide nor iodide ions when incorporated in uranyl sulfate solutions have produced cracking.

Cold-formed type 347 stainless steel pipes have developed stress-corrosion cracks when steam was passed through them and Y-12 chloride-containing potable water was sprayed on their surfaces. Either annealing or shot-peening the pipes after bending prevented cracking during a 1000 hr test, but stress relief treatments between 600 and 1250°F were ineffective. Cold-formed titanium and modified type 430 stainless steel showed no cracking.

A number of different zirconium-base alloys prepared by the HRP Metallurgy Group have been tested in uranyl sulfate solutions. Although all alloys tested showed good corrosion resistance to uranyl sulfate solutions, none of the alloys were as resistant as Zircaloy-2.

Corrosion studies related to the Chemical Processing Plant of the HRT have been primarily concerned with testing stabilized Carpenter 20 stainless steel specimens which are representative of the material being used in actual fabrication of the plant. Most of the tests have been run in boiling 4 M H_2SO_4 to which had been added simulated corrosion and fission products. All specimens have shown adequate corrosion resistance with two exceptions: One specimen showed apparent stress-corrosion cracks and one welded specimen showed knife-line attack and some selective attack of the weld metal itself.

II. INTRODUCTION

The data presented in the following sections represent the detailed results obtained during the past quarter (October 31, 1956 to January 31, 1957) by the out-of-pile solution corrosion group of the Homogeneous Reactor Project. A summary of the data has been reported in the Homogeneous Reactor Project Quarterly Progress Report for the period ending January 31, 1957.

It should be pointed out that the data presented below are, for the most part, preliminary, and the interpretation of the results may change as further experimentation is completed.

III. 100A LOOP PROGRAM (J. C. Griess, H. C. Savage, R. S. Greeley, S. R. Buxton, T. H. Mauney, W. C. Ulrich)

A. Transition Joint Mockup:

A second test of the mockup of the Zircaloy-stainless-steel transition and expansion joint, previously mentioned(1), has been made in 100A dynamic Loop F. A detailed report on the first test was published elsewhere(2).

When the test vessel flanged joint had been reassembled after the first test, the loop was filled with water to the desired volume and brought to temperature; then, concentrated fuel solution was added to give a solution of the following composition: 0.04 m UO_2SO_4, 0.005 m $CuSO_4$, and 0.02 m H_2SO_4.

The thermal cycling was performed as before between 100°C at 100 psig and 300°C at 1550 psig. Mechanical deflections of the bellows through a total traverse of 5/8 in., 5/16-in. extension and 5/16-in. compression relative to the neutral point, were made during each thermal cycle. An additional mechanical deflection of the bellows of 5/8 in., from the fully extended position to fully compressed and return, made in 1/8-in. increments over a period of about 15 min, was imposed during each 16-hr period that the system was at 300°C.

The test was of 1200 hr duration, during which time the bellows underwent 50 complete thermal cycles with mechanical deflection during thermal cycling, and 47 additional mechanical deflections during the time the system was at 300°C. Since installation, the bellows has now been subjected to a total of 104 thermal cycles and 148 mechanical deflections.

A differential pressure across the bellows from outside to inside and across the gasket in the transition joint was maintained at about 45 to

428 004

50 psia. The interior of the bellows was kept full of water from the condensate tank and daily samples of the water were taken in order to detect any leakage of the fuel solution across the test gasket or the expansion joint. No leakage across the transition joint or expansion bellows was detected at any time during the run. At the end of the run the housing surrounding the test assembly was removed and an additional leak test was made by applying 50 psig of helium inside the expansion joint and bellows and "sniffing" the exterior with a mass-spectrograph-type leak detector. No leakage was detected.

Prior to disassembly, the 10-in., IPS, 1500-lb test vessel oval-ring joint was leak tested at 200 psig of helium with a mass-spectrograph-type leak detector. No leakage was observed.

Examination of the bottom groove of the 10-in.-IPS flange showed that no leakage of solution into the groove had occurred; in contrast, leakage had occurred into the bottom groove during the previous test(3). The oval-ring gasket was removed from the flange top groove for the first time since the original assembly. No solution leakage had ever occurred into the toop groove. The oval-ring gasket was examined with a 10X microscope and no significant attack was apparent.

The pitted areas on the bellows at the edges of the reinforcing rings, mentioned previously(4), were examined closely by moving the rings to reveal the entire crevice area between the rings and the bellows. Figure 1 illustrates the appearance of the pits after the first run and after the second run. As can be seen, one new pit developed at the edge of the top ring during the second run (No. 6) and two small pits (No. 2 and 3) spread into a long collection of pits (No. 1, 2, 3, and 4). The pitting at the lower edge of the bottom ring did not continue during the second run.

The depth of the pits was measured with a microscope-dial gauge indicator assembly by focusing the microscope on the edge of a pit and then on the bottom of the pit and noting on the dial indicator the microscope carriage travel. Although this method gave pit depths accurate to only ± 0.002 to 0.003 in., the following conclusions were drawn:

1. The average pit depth at the edge of the top ring roughly doubled during the second run. The pitting at the lower edge of the bottom ring did not continue.
2. The pit depth increased from 0.008 to 0.016 in. to about 0.015 to 0.020 in. with one pit giving an average depth measurement of 0.023 in.(5).
3. The rate of pitting attack on those areas pitted in the first test remained approximately the same as in the first test, about 100 mpy, even though the frequency and total number of mechanical deflections of the bellows were doubled in the second run. However, the newly pitted areas (No. 1, 4, and 6 in Figure 1) appeared to be almost as deep as the previously pitted areas, indicating an attack rate on the new areas substantially higher than 100 mpy.

ORNL-LR-Dwg.-19438
UNCLASSIFIED

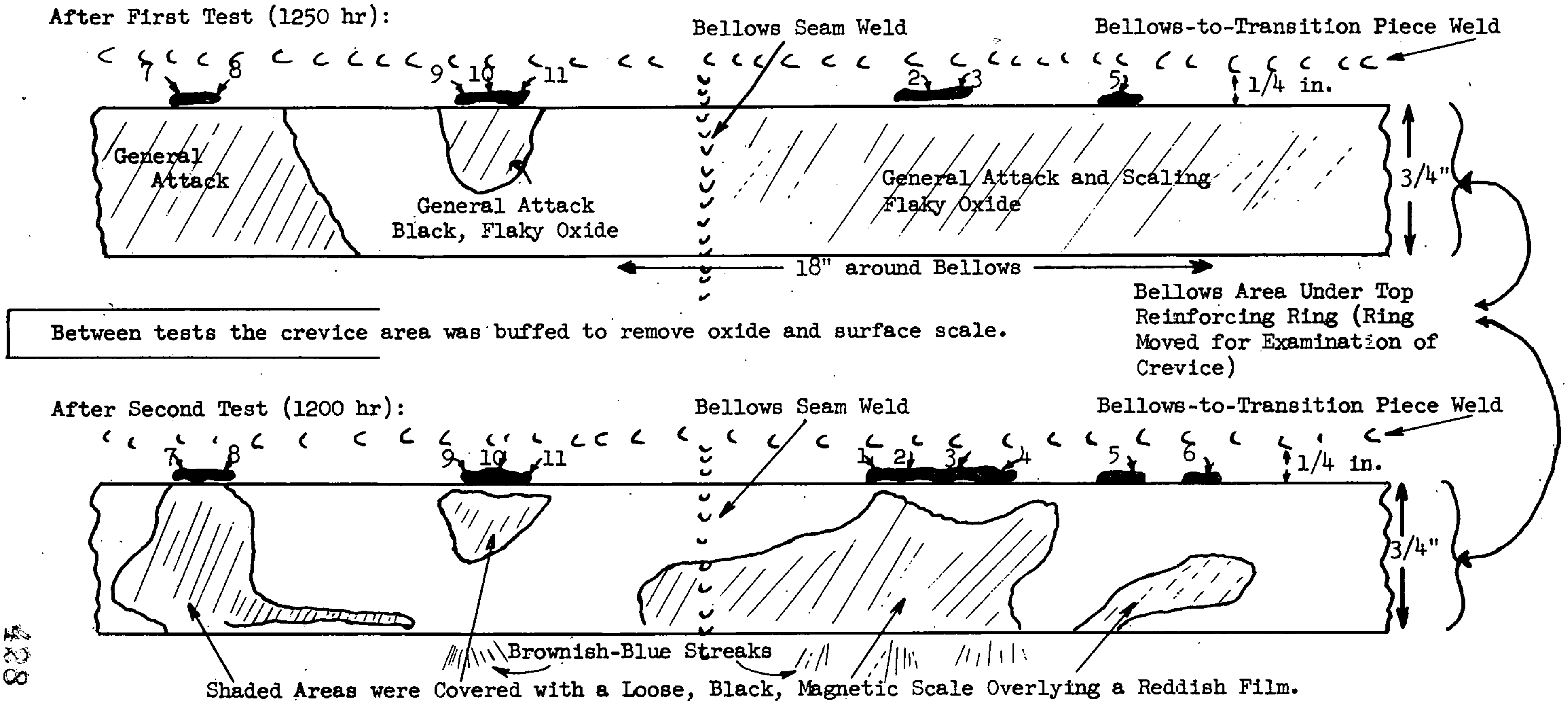

Average Pit Depth in Pitted Areas (Shaded Black Above):

	After First Test	After Second Test
No. 1	Not Attacked	0.015 in.
No. 2	0.008 in. max.	0.019 in.
No. 3	0.008 in. max.	0.019 in.
No. 4	Not Attacked	0.014 in.
No. 5	0.008 in. max.	0.016 in.
No. 6	Not Attacked	0.018 in.
No. 7	0.008 - 0.010 in.	0.019 in.
No. 8	0.008 - 0.010 in.	0.023 in.
No. 9	0.013 in.	0.020 in.
No.10	0.016 in.	0.017 in.
No.11	0.013 in.	0.013 in.

Figure 1: Appearance of Area Under Top Reinforcing Ring on HRT Core-Pressure Vessel Bellows Mockup After Operation in Simulated Fuel Solution.

4. Pitting attack did not occur in the crevice between the reinforcing rings and the bellows but originated about 1/32 to 1/16 in. above the top ring and below the bottom ring. Thus, the pitting did not appear to be due strictly to crevice corrosion but to a combination of effects not yet understood. Attack in the crevice area was general and slight.

The corrosion specimens in the main loop were removed, scrubbed, and weighed. They were not defilmed but were replaced in the loop for further testing. As before(6), the pins exposed at low flow rate (17 fps) showed slight weight gains in the scrubbed condition, indicating essentially no corrosion during this second test. Alloys exposed included titanium RC-55, Zircaloy-2, Incoloy, and types 347, 304L, and 309 SCb stainless steel.

The pins exposed at high flow rate (70 fps) were either titanium or zirconium alloys. Commercially pure titanium crystal bar zirconium, and Zircaloy-2 again showed insignificant weight losses, but the alloys of titanium with aluminum and tin, aluminum and vanadium, aluminum and manganese, and aluminum and chromium showed definite, though small, weight losses. The corrosion rates of the above-named alloys were between 0.5 and 1 mpy (scrubbed).

The type 347 stainless steel coupons showed weight gains in the scrubbed condition after the second test, except the last one exposed at 50 - 64 fps. It was very badly attacked with an average corrosion rate of 73 mpy. The critical velocity was very sharp at 50 fps. This was at least as high as that observed in a similar test without thermal cycling(7).

Specimens of the following alloys were suspended in the solution inside the bellows test unit and exposed to a flow rate of less than 1 fps: types 347, 304L, and 309 SCb stainless steel, titanium RC-55, titanium - 8% manganese, titanium - 6% aluminum - 4% vanadium, crystal bar zirconium, and Zircaloy-2. These were removed after the second test, scrubbed, and weighed. They were not defilmed but were replaced in the test unit for further testing. The zirconium alloys and the type 304L stainless steel specimens showed slight weight gains as-scrubbed; the other stainless steels and the titanium alloys showed small weight losses. All of these specimens were filmed over. Microscopic examination showed on several of the type 347 and 309 SCb stainless steel specimens a few small pits in the crevice area where they had been bolted to the holder. These pits definitely originated underneath the bolt head and thus were unlike the pits observed on the bellows. The pits on the specimens appeared to be relatively shallow (less than 10 mils deep) and the attack appeared to have stifled itself.

Other specimens of type 347 stainless steel, titanium 75A, and Zircaloy-2, mounted inside the bellows test unit in contact with one another to investigate crevice and galvanic couple attack, and stressed specimens of type 347 stainless steel, titanium - 6% aluminum - 4% vanadium, and Zircaloy-2 were examined under a 10X microscope but were not disassembled or weighed. They were returned to the test unit for further testing. Visually, these specimens had not suffered significant attack and no effect of galvanic coupling, crevice, stress, or thermal cycling was noted.

The increase in nickel(II) ion concentration in solution indicated a generalized corrosion rate of about 0.3 mpy. This was roughly one-third less than observed in the first test(8) but still was about three times higher than in a similar test made without thermal cycles(7). The solution was stable throughout the run.

B. Runs with Uranium Trioxide Dissolved in Beryllium Sulfate Solutions:

It was reported previously that beryllium sulfate solutions will dissolve appreciable quantities of uranium trioxide and that the resulting solutions have a higher pH at room temperature than uranyl sulfate solutions containing the same concentration of uranium(9). Since it was felt that solutions of the same uranium concentration would be less corrosive the higher the pH, runs were made with 0.04, 0.17, 0.25, and 0.36 m UO_3 dissolved in various beryllium sulfate solutions; the corrosion results were compared with those obtained in uranyl sulfate solutions. All runs were made in Loop "O" which is especially shielded and vented for safe handling of beryllium solutions.

Properties of the beryllium-containing solutions are listed in Table I. All solutions were stable up to the temperature of appearance of a second liquid phase when observed in quartz tubes. In the loop, the solutions were stable to ± 10 percent with two exceptions: The 1.0 m $BeSO_4$ solution with 0.36 m UO_3 gave a slight precipitate of beryllium oxide and uranium trioxide in 200 hr at 250°C (run No. 6): and the 0.2 m $BeSO_4$ with 0.04 m UO_3 and 0.005 m $CuSO_4$ lost nearly 30 percent of its beryllium (presumably as beryllium oxide) and the pH decreased 1.6 units in 200 hr at 280°C (run No. 9).

TABLE I

Properties of Uranium Solutions Containing Beryllium Sulfate

Run No.	Concentration $BeSO_4$	Concentration Uranium as UO_3	Concentration $CuSO_4$	pH at 28°C	Temperature of Appearance of 2nd Liquid Phase	Remarks
3	1.0 m	0.17 m	-	2.8	302°C	Stable 87 hr at 250°C.
5	1.0 m	0.25 m	-	3.1	~290°C(a)	Stable 176 hr at 250°C.
6	1.0 m	0.36 m	-	3.3	278°C	Slight Precipitation of BeO and UO_3 occurred in 200 hr
7	0.5 m	0.17 m	-	3.5	275°C	Stable 177 hr at 250°C
8,9	0.2 m	0.04 m as UO_2SO_4	0.005 m	3.4	295°C	Precipitation of Be and decrease in pH occurred at 280°C in 200 hr
10,11	0.04 m	0.04 m	0.005 m	2.8	317°C	Stable 200 hr at 300°C.

(a) Interpolated value.

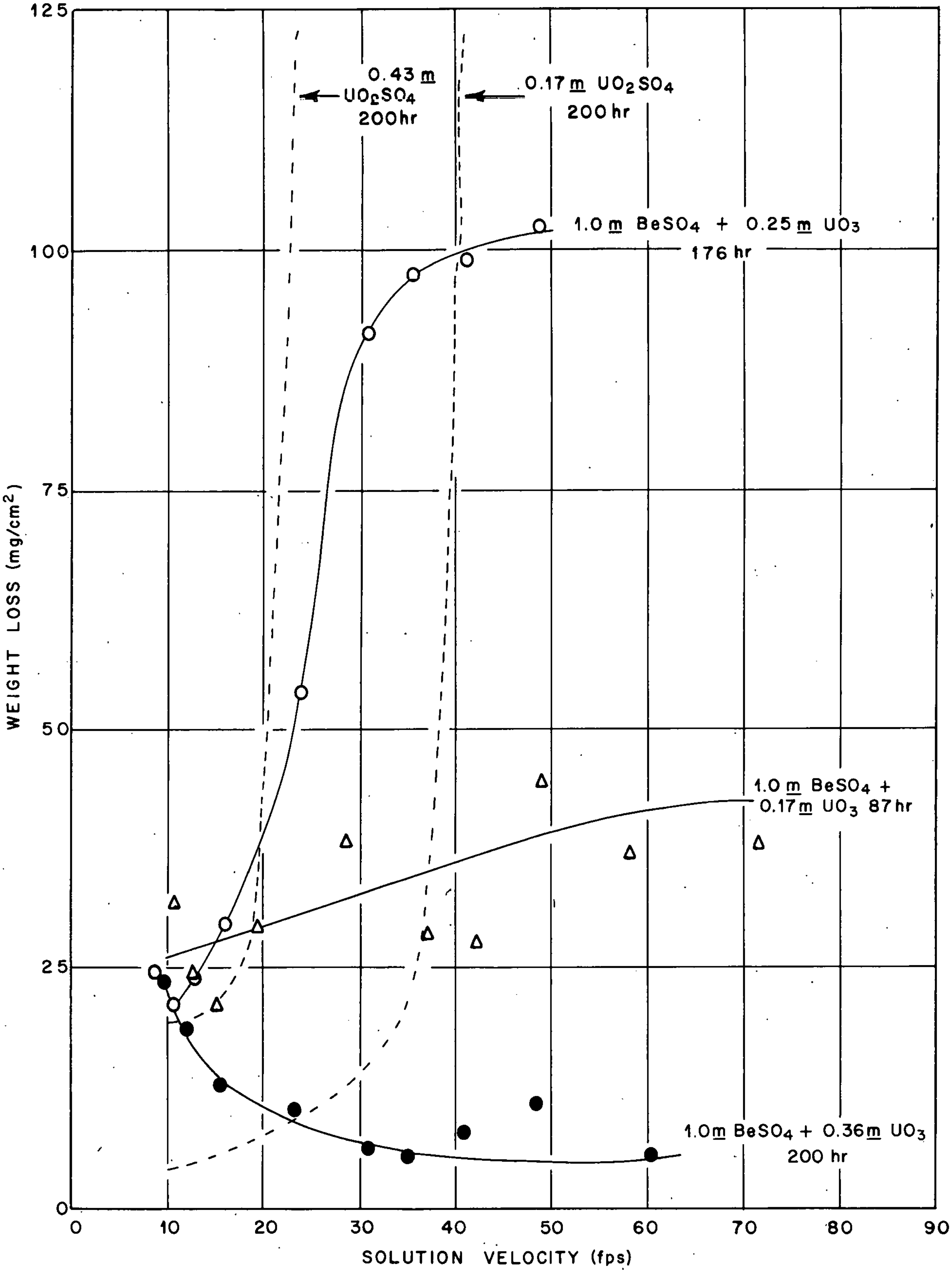

Fig. 2 Comparison of Weight Losses of Type 347 Stainless Steel Coupons in UO_3-$BeSO_4$ Solutions and in UO_2SO_4 Solutions at 250°C

Corrosion results with the 1.0 m and 0.5 m $BeSO_4$ solutions were erratic and not as low as anticipated. Figure 2 illustrates these coupon results and for comparison shows also the average results obtained in 0.17 m and 0.43 m UO_2SO_4 solutions under similar conditions. The weight losses of the type 347 stainless steel coupons in 1.0 m $BeSO_4$ with 0.17 m UO_3 showed no regular velocity dependence, whereas with 0.25 m UO_3 a sharp critical velocity at 10 to 15 fps was observed; with 0.36 m UO_3 weight losses decreased with increasing velocity.

As can be seen, weight losses at low velocities were as great or greater in the uranium trioxide - beryllium sulfate solution as in the uranyl sulfate solution but at high velocities were significantly less. The very low results in 1.0 m $BeSO_4$ with 0.36 m UO_3 may not be accurate since some hydrolytic precipitation of uranium and beryllium occurred (perhaps as much as 20%). A run not shown in Figure 2, in which 0.17 m UO_3 was dissolved in 0.5 m $BeSO_4$, showed that corrosion of stainless steel was less at the lower beryllium sulfate concentration. However, low velocity weight losses were still greater than in 0.17 m UO_2SO_4. Solutions of 0.17 m UO_3 in beryllium sulfate less than 0.5 m were not stable at 250°C.

Approximately 0.2 m $BeSO_4$ was necessary to dissolve sufficient uranium trioxide to give a solution containing 0.04 m uranium, the concentration proposed for use in the HRT. Therefore, runs were made with 0.2 m $BeSO_4$ containing 0.04 m UO_3 and 0.005 m $CuSO_4$ at 250 and 280°C (Run 0-8 and 0-9). Higher temperatures were not studied since the solution separated into two liquid phases at 295°C. In addition, even at 280°C, the solution was not completely stable as shown by the fact that some beryllium was lost from solution during the 200 hr run. The weight losses of the type 347 stainless steel coupons are shown in Figure 3; included on the same figure are runs made with 0.04 m UO_2SO_4 containing 0.02 m H_2SO_4 and 0.005 m $CuSO_4$ for comparison. The composition of the latter solution is the same as that to be used in the HRT.

It can be seen that generally the results in the 0.04 m UO_3-0.2 m $BeSO_4$ solution were worse than in the 0.04 m UO_2SO_4 solution containing 0.02 m H_2SO_4, although the difference at 250°C was not great. Therefore, it is felt that solutions of uranium trioxide in beryllium sulfate offer no advantage over uranyl sulfate solutions in the range 0.04 to 0.17 m uranium as far as out-of-pile corrosion of stainless steel is concerned at 250°C. Possibly, at lower temperatures, the uranium trioxide-beryllium sulfate system may offer some advantages over the uranyl sulfate system.

C. Runs with Dilute Equimolal UO_2SO_4-$BeSO_4$ Solution:

Dilute solutions of uranyl sulfate with equimolal lithium, sodium, or magnesium sulfate have been shown to be unstable in regard to precipitation of uranium at 300°C(10). However, since beryllium sulfate solutions are acidic, it was felt that dilute equimolal uranyl sulfate-beryllium sulfate solutions would be stable up to 300°C. A solution of 0.04 m UO_2SO_4 containing 0.04 m $BeSO_4$ and 0.005 m $CuSO_4$ was stable in a quartz tube at 300°C for 3 hr and had a two-liquid phase separation temperature of 317°C (see Table I runs "0"-10 and 11).

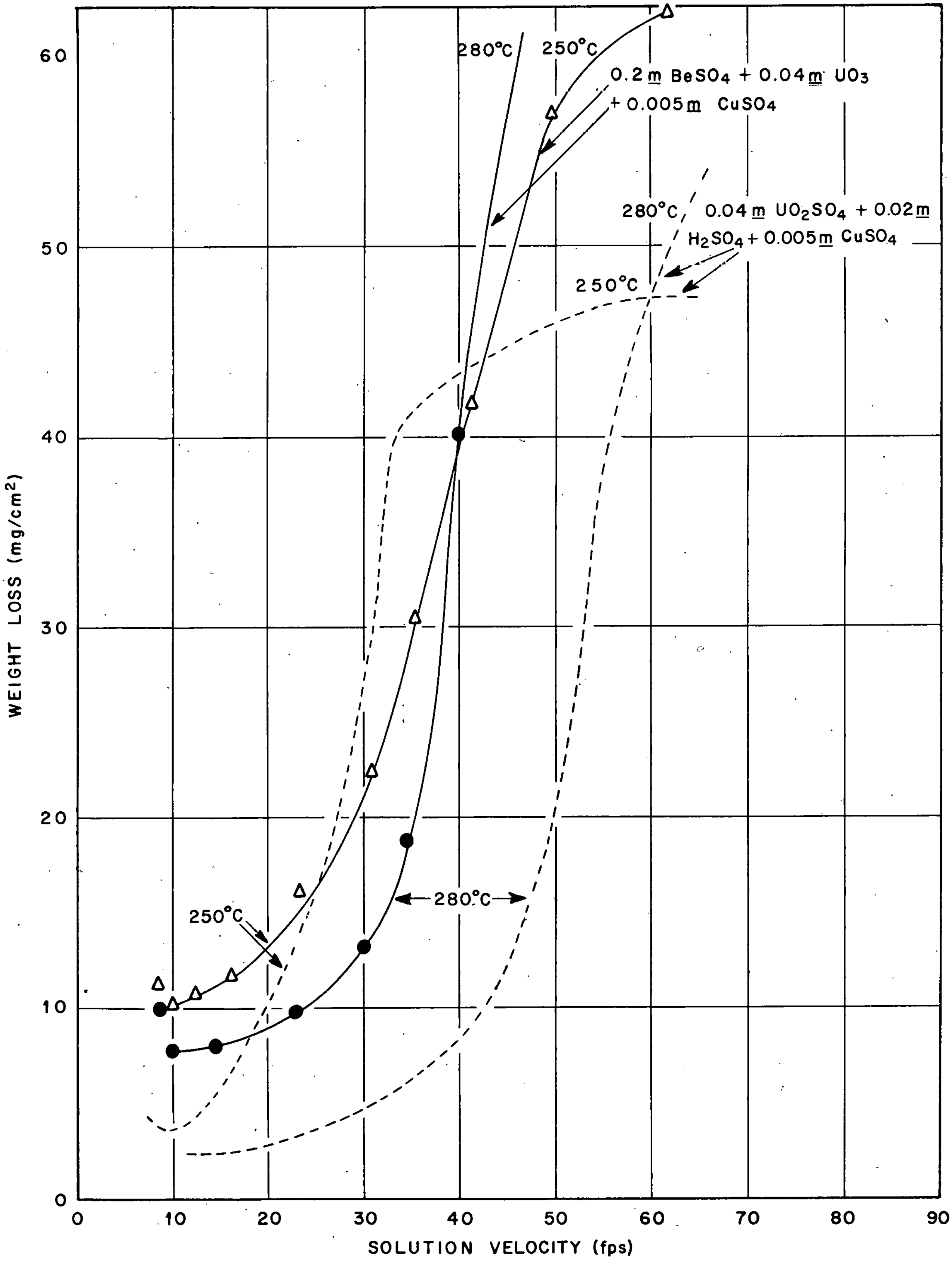

Fig. 3 Comparison of Weight Losses of Type 347 Stainless Steel Coupons in UO_3 - $BeSO_4$ Solutions and in UO_2SO_4 Solutions (200 hr runs)

Two runs have been made with this solution: one at 300°C for 200 hr and one at 250°C for 200 hr. The corrosion results were similar to those observed in 0.04 m UO_2SO_4 solution containing 0.02 m H_2SO_4 + 0.005 m $CuSO_4$. The weight losses of the type 347 stainless steel coupons are plotted in Figure 4 and are compared with results obtained in 0.04 m UO_2SO_4 solution with 0.02 m H_2SO_4 and 0.005 m $CuSO_4$. The solution in both runs was stable, although longer runs might show a slow hydrolytic precipitation since room temperature pH decreased 0.2 to 0.3 units during each run.

The room temperature pH of a solution containing 0.04 m UO_2SO_4, 0.02 m H_2SO_4 and 0.005 m $CuSO_4$ is 1.5, whereas a solution containing 0.04 m $BeSO_4$ and 0.04 m UO_2SO_4 is 2.8. Since both solutions appear to be stable at high temperatures, it is possible that the temperature dependence of the beryllium sulfate hydrolysis is such that the hydrolysis supplies the acid necessary to stabilize the uranyl sulfate. Thus, at high temperature where more acid is needed to stabilize the uranyl sulfate, the degree of hydrolysis of beryllium sulfate would be greater than at low temperatures where less acid is necessary. If the above reasoning is correct, it would be expected that the equimolal uranyl sulfate-beryllium sulfate solution would be less corrosive in the range of 150 to 250°C than a uranyl sulfate solution containing sulfuric acid. Tests to determine the accuracy of the above hypothesis are in progress.

D. Long-Term Runs with Proposed HRT Solution:

1. Isothermal Runs at 200, 250, and 300°C.

The long-term runs at 200, 250, and 300°C with the solution proposed for use in the HRT (0.04 m UO_2SO_4, 0.02 m H_2SO_4, and 0.005 m $CuSO_4$) were terminated after 3681, 3660, and 3841 hr, respectively.

The solution was hydrolytically stable in all of the runs. However, at 300°C, after 2740 hr, a sudden unexplained decrease in copper ion concentration of about 12% occurred. After this decrease, the copper ion concentration remained constant. Since the loss in copper was not accompanied by a decrease in pH or uranium concentration, it seems unlikely that hydrolysis was responsible for the loss.

Table II lists the corrosion rates determined both from the final weight loss averaged over the entire run (over-all corrosion rate) and from the difference between the intermediate and final scrubbed weight (continuing corrosion rate). The former indicated the extent of total attack. The latter represent the continuing corrosion rate after film formation and show that all of the stainless steel pins were exposed below their critical velocity, except those at 34 and 42 fps at 200°C. Comparing the two sets of rates, it can be seen that the total attack was relatively severe at 8 to 12 fps at 200°C and at 20 to 34 fps at 250°C, even though the pins eventually filmed over and stopped corroding. On the other hand, the continuing corrosion rates at 34 to 42 fps at 200°C were lower than the over-all rates showing that the film was partially protective above the critical velocity.

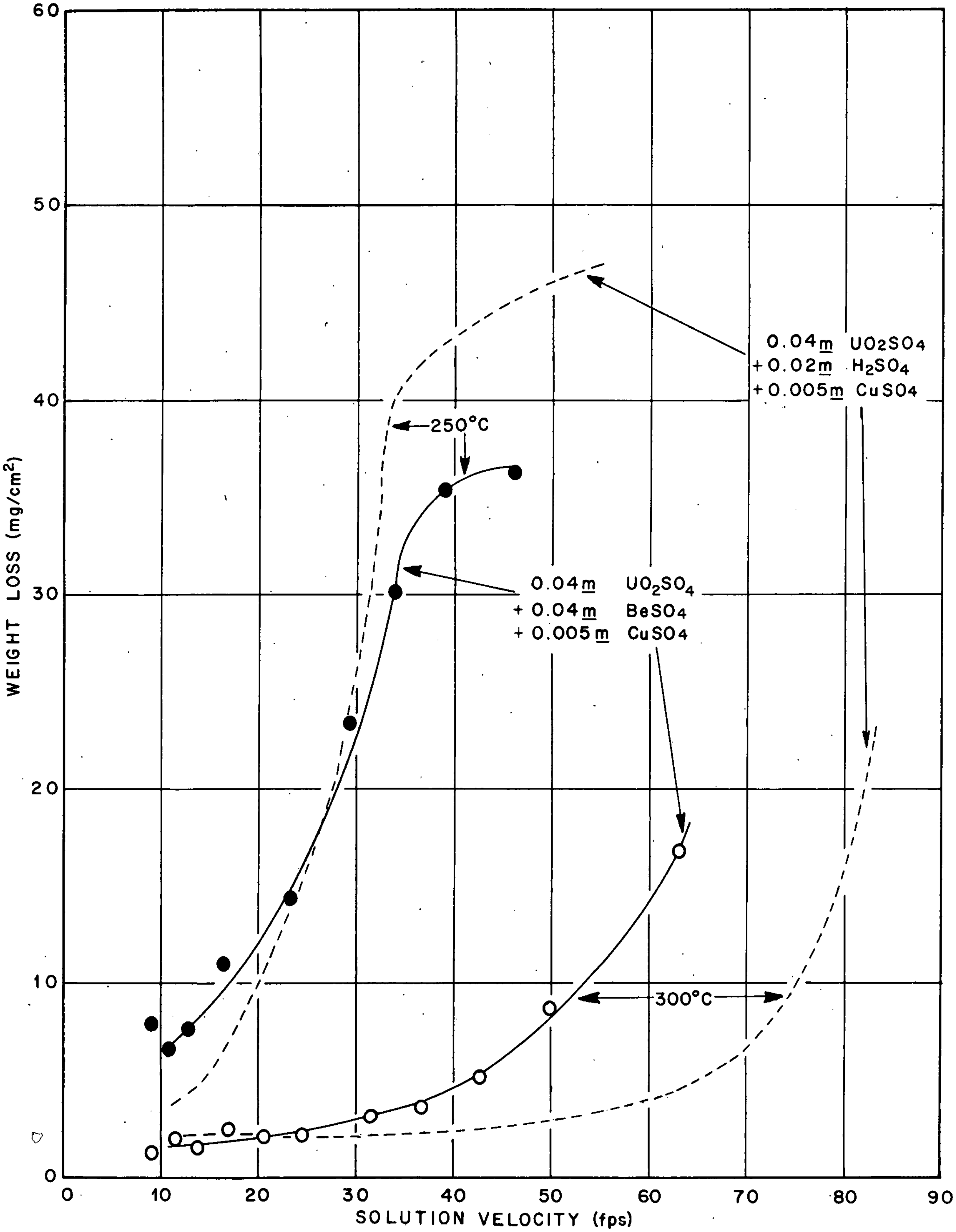

Fig. 4 Comparison of Weight Losses of Type 347 Stainless Steel Coupons in UO_2SO_4 - $BeSO_4$ Solution and in UO_2SO_4 - H_2SO_4 Solution (200 hr runs)

TABLE II

Corrosion Rates in Long Term Runs with 0.04 m UO_2SO_4 + 0.02 m H_2SO_4 + 0.005 m $CuSO_4$, 500 - 1500 ppm O_2

Materials	Flow Rate (fps)	Over-all Corrosion Rates (mpy) 200°C (3683 hr)	250°C (3660 hr)	300°C (3841 hr)	Continuing Corrosion Rates (mpy) Based on Scrubbed Weights 200°C (1876-3683 hr)	250°C (1854-3660 hr)	300°C (2020-3841 hr)
Ave. Stainless Steels (new pins)[(a)]	8	1.7	-	-	0	-	-
	12	4.9	0.75	0.23	0	0	0
	20	-	1.1	0.31	-	0	00
	26	-	0.93	0.42	-	0	0
	34	12	1.3	0.47	5.4	0	0
	42	16	-	-	8.0	-	-
Niobium	8	0.01	-	-	0	-	-
	12	-	0.35	-	-	0.39	-
	34	-	0.81	-	-	0.80	-
	42	5.4	-	-	5.0	-	-
Titanium[(b)]	8-42	0	0	0	0	0	0
Zirconium[(c)]	8-42	0	0	0.05	0	0	0
Titanium[(d)]	20-34	0	0.09-0.18	0.33-0.42	0	0.08-0.10	0.13-0.35

(a) Includes types 304, 304 cast, 304 sensitized, 304 L, 309 SCb, 347 347 cast, 347 Sensitized, 430, and 446.

(b) Includes types RC-55, 75A, 100A, and 150A.

(c) Includes crystal bar zirconium, zirconium - 2-1/2% Sn, and Zircaloy-2.

(d) Includes titanium - 3% Al, 5% Cr, Ti - 6% Al, 4% V, Ti - 5% Al, 2-1/2% Sn, and Ti - 4% Al, 4% Mn.

The previous report(11) gave several qualitative observations from an examination of the specimens in the scrubbed condition part way through the runs. Final examination of the specimens, some scrubbed and some defilmed, supported these observations:

a. All of the pins that had been exposed in previous runs with less agressive environments were protected by the previously formed films and gained weight even above the critical velocity on new stainless pins (e.g., 36 and 42 fps at 200°C).

b. New stainless steel pins corroded more during the period of film formation than in previous runs with less acid.

c. New stainless steel coupons, exposed in these runs only, indicated critical velocities of 15 to 20 fps at 200°C, 25 to 30 fps at 250°C and 35 to 40 fps at 300°C. However, a second set of coupons exposed during the last part of the run at 250°C showed a higher critical velocity, 30 to 35 fps, which was more nearly that shown by the pins. Also, the second set showed less dependence of corrosion on velocity than the first set and higher low-velocity weight losses. Thus, it appears that changes in the solution with time, perhaps in particular, the increase in chromium(VI) concentration, can appreciably affect the corrosion rate and critical velocity of stainless steel.

d. Titanium and zirconium alloys showed excellent corrosion resistance. Niobium at 8 fps at 200°C appeared to film over, but at higher velocities at 200 and 250°C remained film-free and corroded at rates as high as 5 mpy.

e. Stress-corrosion specimens(11) after a total exposure of 9000 hr, showed no evidence of stress-corrosion cracking. The chloride concentration was less than 3 ppm throughout the runs.

2. Run at Successively Increased Temperature.

An additional run in which 0.04 m UO_2SO_4 containing 0.02 m H_2SO_4 and 0.005 m $CuSO_4$ was circulated at temperatures ranging from 175 to 300°C was also completed. Prior to the run, the system was defilmed with a chromous sulfate solution(12) in order to study how corrosion rates of new stainless steel specimens would change with temperature in an essentially new stainless steel system. Table III shows the operating temperatures for the run. The corrosion specimens were defilmed only at the conclusion of the run; the corrosion rates of the specimens during each period of operation were calculated from weight changes in the "as-removed" condition in order to show what would happen at each higher temperature to a surface that became filmed over at low temperatures on start up.

At 200 to 225°C, corrosion rates up to 5 mpy were observed for stainless steel pins at 23 fps and up to 23 mpy for stainless steel coupons and pins at 44 to 50 fps. Corrosion rates at 175°C were about the same as at 250°C, being no higher than 2 mpy at 23 fps and 9 mpy at 50 fps. Corrosion rates at all velocities at 300°C were between 2 and 4 mpy, and it is possible that this represents not loss of metal but a dehydration or other change in the character of the film at high temperature. Figure 5 illustrates the change in corrosion rates of types 304 L, 321, and 347 stainless steel pins with temperature. Titanium and zirconium pins showed insignificant attack throughout the run.

This run at successively higher temperatures may be compared in a qualitative way with the isothermal runs discussed above as follows:

a. Corrosion of stainless steel was relatively severe above the critical velocity in both cases.

b. The critical velocity at each temperature in this run was roughly the same as in the isothermal run at the same temperature.

Therefore, it was concluded that exposure of stainless steel to this solution at one temperature does not significantly affect corrosion at a higher temperature. In other words, the corrosion results from the isothermal runs are also valid for conditions of successively increased temperatures.

TABLE III

Operating Conditions During Run at Various Temperature

Solution: 0.04 $\underline{m}$ UO_2SO_4, 0.02 $\underline{m}$ H_2SO_4, 0.005 $\underline{m}$ $CuSO_4$, 500-1000 ppm O_2

Time (hr)	Temp. °C	Remarks
440	175	Run interrupted after 292 hr at 175°C to examine corrosion specimens.
1702	200	Run interrupted after 573 hr at 200°C to examine specimens.
1734	225	
366	250	
339	300	

3. Run Using Heavy Water Solution.

The stability of the proposed HRT solution in heavy water instead of normal water has also been investigated since the HRT will use a heavy water solution. A solution containing 0.04 $\underline{m}$ UO_2SO_4, 0.02 $\underline{m}$ D_2SO_4 and 0.005 $\underline{m}$ $CuSO_4$ was circulated for 1000 hr at 300°C. The solution was stable and corrosion results were similar to those obtained in light water solution(7). Thus, there does not appear to be an observable isotope effect in the corrosion and hydrolysis reactions occurring in these experiments.

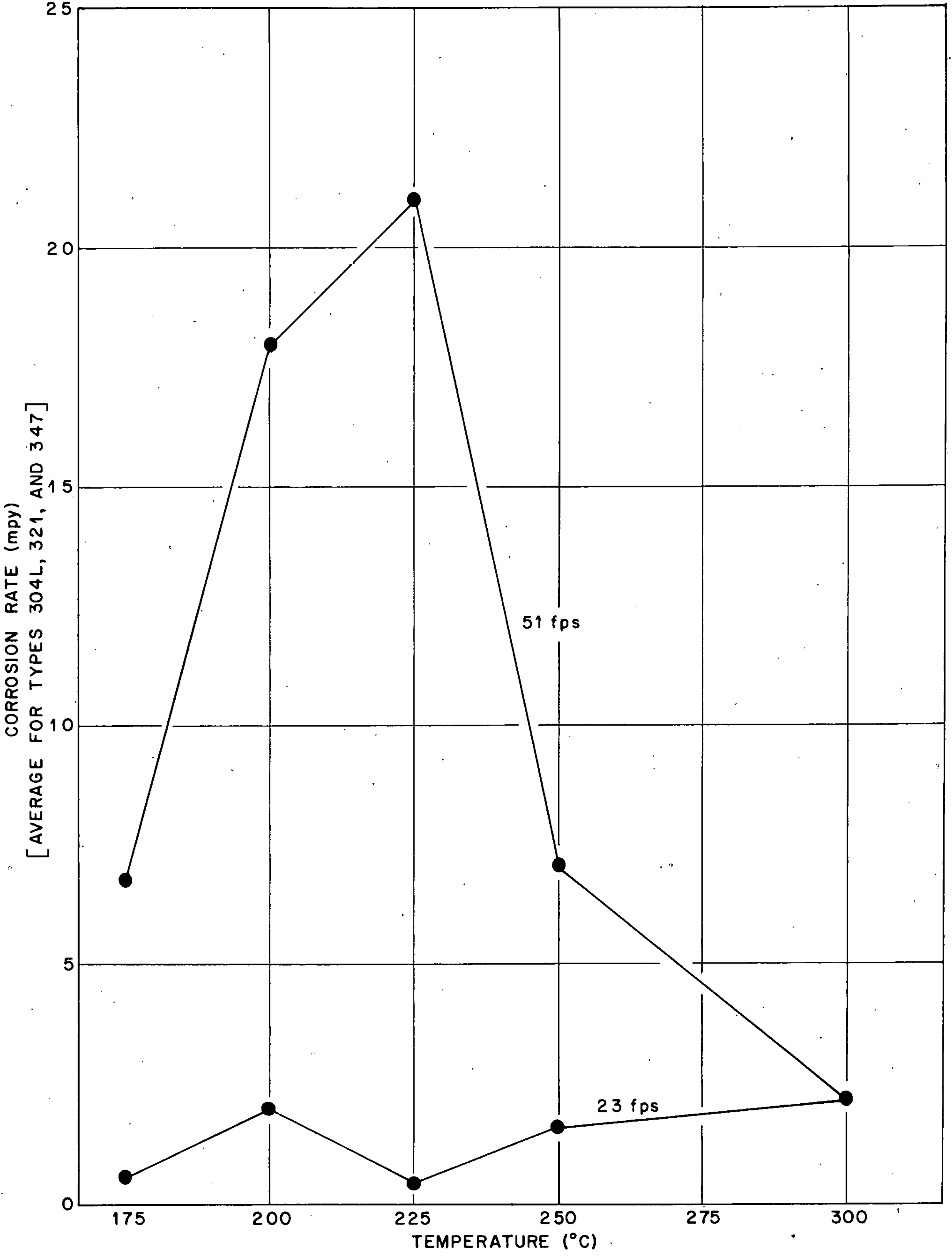

Fig. 5 Effect of Temperature on Corrosion Rates of Stainless Steel Pins in 0.04 m UO_2SO_4 + 0.02 m H_2SO_4 + 0.005 m $CuSO_4$

E. Effect of Chromium(VI) at 300°C on the Corrosion of Stainless Steel in 0.17 m Uranyl Sulfate Solution:

In the last report(13), data were presented on the effect of chromium(VI) in uranyl sulfate solutions on the corrosion of stainless steel at 250° and 275°C. During the past quarter, a similar study was made at 300°C. The experimental conditions were the same as in the previous studies; all runs were made in the titanium loop, Loop G, for 100 hr in 0.17 m UO_2SO_4 containing about 1000 ppm oxygen. Two type 347 stainless steel pins were exposed at 10 to 12 fps where a film formed, and two, at 68 to 70 fps where a protective film did not form.

The results obtained at 300°C, as well as those at 250 and 275°C are shown in Figure 6. Because the pins exposed at 300°C at high velocity were partially filmed over on the downstream side, micrometer measurements instead of weight losses were used to determine the depth of penetration on the film-free portions of the pins. The filmed-over corrosion rate in the low flow region was lower than those obtained at 250°C and 275°C and the high velocity corrosion rates were higher. The scatter of the points at the higher flow rate was probably due to errors in the micrometer readings.

Since the data reported above parallel previously reported data, the same mechanism as presented before seems to be applicable(14). An Arrhenius activation energy plot was made (log corrosion rate versus reciprocal absolute temperature) at constant chromium(VI) concentration for corrosion rates at 70 fps. Although the data are scattered, an apparent activation energy of about 16 kilocalories per mole was calculated from the slope of the best straight line through the points at zero and at 10 ppm Cr(VI) added. This value for the activation energy for corrosion is in rough agreement with those determined previously(15), showing that Cr(VI) does not affect the mechanism of the corrosion reaction.

F. Effect of Copper(II) Concentration at 250°C on the Corrosion of Stainless Steel in 0.17 m UO_2SO_4.

The effect of the addition of various amounts of cupric sulfate to 0.17 m UO_2SO_4 at 250°C on the corrosion of type 347 stainless steel has been studied in three runs. Each run was of 100 hr duration and was made in the all-titanium loop, Loop G, with an oxygen concentration of 1000-2000 ppm. The results are shown in Table IV, which also includes for comparison, data from a previous run, G-44, which was made under the same experimental conditions with no cupric sulfate added.

The data show that 49 ppm copper(II) had no apparent effect on the corrosion of type 347 stainless steel pins in either the low or high flow regions. However, increasing the copper(II) concentration to 290 ppm increased the high velocity corrosion rate slightly, but had no measurable effect on the low velocity corrosion rate. When the copper(II) concentration was raised to 1150 ppm, the corrosion rate at low velocity was not significantly different from those rates observed in tests with lower copper(II) concentrations. The corrosion rate at high velocity increased.

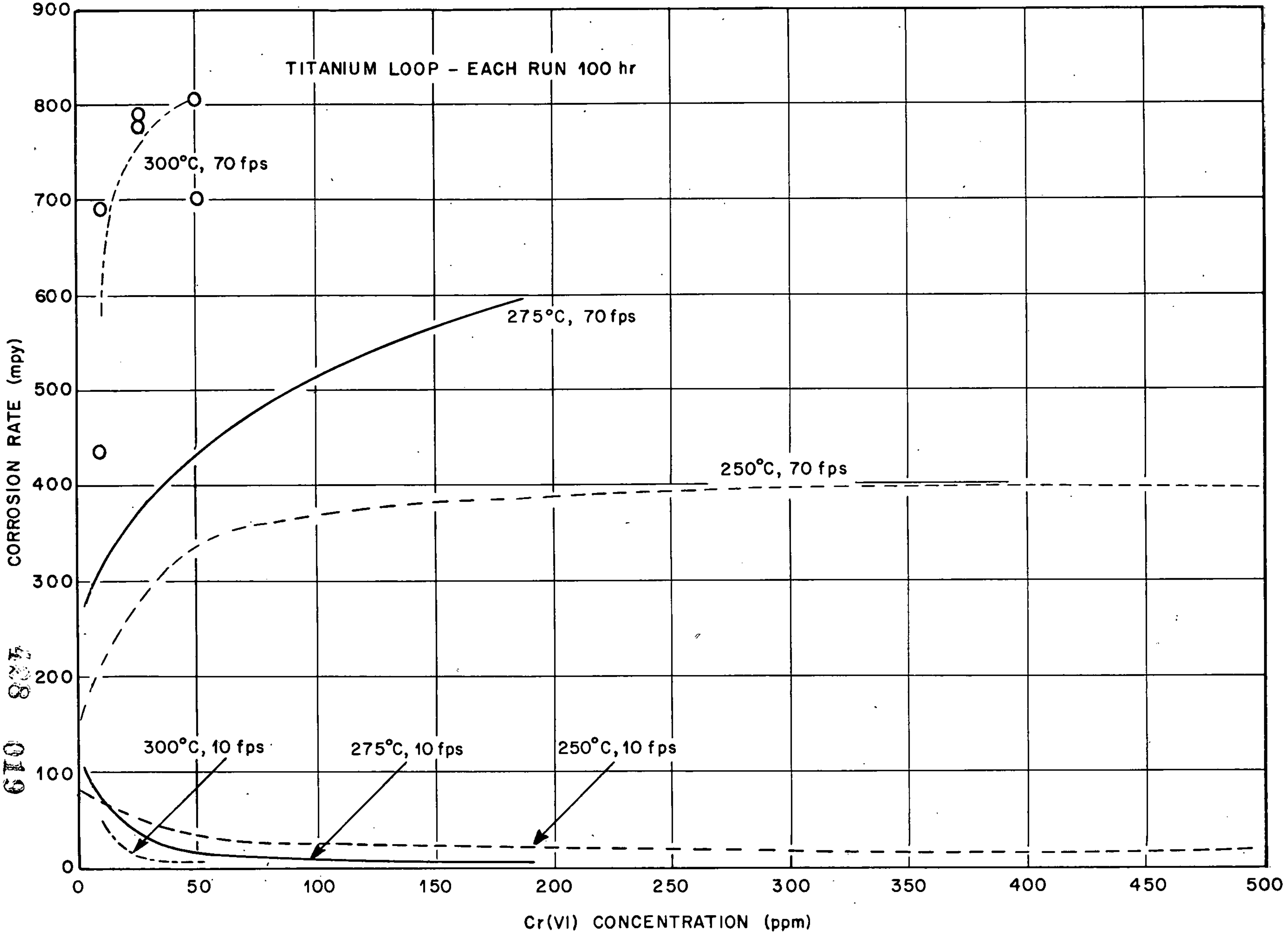

Fig. 6 Corrosion of Type 347 SS Pins in 0.17$\underline{m}$ UO_2SO_4 Containing Cr(VI)

ORNL-LR-Dwg.-19443
UNCLASSIFIED

TABLE IV

The Corrosion of Type 347 Stainless Steel at 250° in 0.17 m UO_2SO_4 Containing Copper Sulfate

Run No.	Cu(II) ppm	Flow Rate fps	Corrosion Rate* mpy
G-44	0	12	85
		12	83
		71	140
		71	180
G-65	49	13	78
		13	83
		68	150
		68	140
G-67	290	13	82
		13	75
		68	200
		68	150
G-68	1150	13	96
		13	99
		68	250
		68	250

* Average Corrosion Rate for 100 hr Run.

G. Corrosion of Bearing Materials by Uranyl Sulfate Solution:

A comparison of the corrosion behavior of various possible bearing materials has been made. The bearing materials were exposed as pin-type specimens to a solution containing 0.04 m UO_2SO_4, 0.02 m H_2SO_4, 0.005 m $CuSO_4$, and 1000-2000 ppm oxygen at a flow rate of 13 fps for 200 hr at 150°C. The temperature of the test and solution flow rate were not typical of bearing environment, but were chosen in order to give corrosion rates high enough to separate the different materials. The results of the experiment are given in Table V

TABLE V

Corrosion Rates of Bearing Materials in 0.04 m UO_2SO_4 containing 0.02 m H_2SO_4 and 0.005 m $CuSO_4$

Temperature - 150°C Time - 200 hr Flow Rate - 13 fps

Materials	Corrosion Rate* mpy
17-7 PH "Annealed" (hardness RC-44)	2.4
17-7 PH Hardened (hardness RC-43)***	25
17-4 PH Annealed (hardness RB-72)	4.1
17-4 PH Partially Hardened (hardness RC-35)	8.1
17-4 PH Fully Hardened (hardness RC-44)***	4.8
Stellite 1	6.1
Stellite 6	5.9
Stellite 98M2	40
Al_2O_3 Sintered (pure alumina)	12
Graphitar -14	81**

*Average Corrosion Rate for the 200 hr Period. ***Pins Cracked During Run

**Pins broke during Removal from Holder

The relatively high corrosion rates of the 17-7 PH hardened and the Stellite 98M2 pins were anticipated(16). The high rate for graphitar was at least partially due to the fact that the pins were broken during removal from the holder and undoubtedly, some graphitar was lost.

Both hardened 17-7 PH pins and both fully hardened 17-4 PH pins developed cracks at the ends where identification numbers were stamped. The cracking of fully hardened 17-4 PH Stainless steel in uranyl sulfate solution has been observed previously(17). The 17-4 PH and 17-7 PH "annealed" pins and the partially hardened 17-4 PH pins did not show cracks under microscopic examination.

The "annealed" 17-7 PH pins had hardness values higher than the hardened 17-7 PH pins. Since 17-7 PH stainless steel may be hardened either by heat treating at 1400°F or by cold working, it is believed that the stock from which the "annealed" pins were made may have become hardened during a preliminary swaging operation either by final annealing at too low a temperature or by swaging without final annealing.

The fact that the 17-7 PH "annealed" pins did not develop cracks and corroded at a rate a factor of ten lower than hardened pins is significant in that a material of hardness RC-44 which showed low tendency to crack and a low corrosion rate could be very useful. Metallographic examination of the pins is being made.

H. Effect of Pretreatment Films on Corrosion of Stainless Steel in Uranyl Sulfate Solutions.

It has been found that some pretreatment films on stainless steel specimens break down in uranyl sulfate solutions and lead to pitting attack(18), whereas other pretreatment films protect stainless steel from attack by uranyl sulfate solutions for long periods of time(19). To study further the stability of preformed films, stainless steel specimens were pretreated in different ways and the resulting specimens were exposed to uranyl sulfate solutions.

Three pretreating solutions were used: (1) 50 ppm chromium(VI) as potassium dichromate, (2) 50 ppm chromium(VI), and (3) 100 ppm chromium(VI) as chromium trioxide. Each solution was circulated for 100 hr at 250°C with 1000 to 2000 ppm oxygen. After rinsing the pretreating solution from the loop, the corrosion specimens were exposed to 0.17 m UO_2SO_4 at 250°C with about 1000 ppm oxygen to see if the pretreatment film would be protective.

The 50 ppm chromium(VI) as potassium dichromate was relatively ineffective. The critical velocity of the type 347 stainless steel specimens after 200 hr in 0.17 m UO_2SO_4 was about the same as in a run without pretreatment, 20 to 30 fps. The 50 ppm chromium(VI) as chromium trioxide was partially effective since the critical velocity in 0.17 m UO_2SO_4 was 35 to 40 fps. The difference between potassium dichromate and chromium trioxide may lie in the lower pH of the chromium trioxide solution.

The pretreatment with a solution containing 100 ppm chromium(VI) as chromium trioxide was very effective. A pretreatment film about 0.1 mg/cm^2 was laid down on most of the specimens. This film on the type 347 stainless steel coupons extended the critical velocity to 55 to 60 fps and withstood attack by 0.17 m UO_2SO_4 for 1000 hr and by 1.3 m UO_2SO_4 for 100 hr. The ability of this film to withstand attack by the concentrated solution is remarkable inasmuch as the critical velocity in 1.3 m UO_2SO_4 without pretreatment would be less than 15 fps at 250°C.

The preceeding experiments show that preformed films may be useful in extending the critical velocity of the system for sometime. Further experiments are in progress to determine how effective these films will be over extended periods of time and to study the mechanism of film breakdown in cases where it occurs.

I. Titanium Inserts in a Stainless Steel Loop:

During the construction of 100A-loop N, two titanium inserts were installed in turbulent regions to protect the stainless steel piping from excessive attack and to investigate crevice attack between the titanium and the steel(20). At the end of Run N-24, after 9900 hr of exposure at 175 to 300°C to 0.04 to 1.3 m UO_2SO_4 solutions, the inserts were cut out for examination. The position of the inserts in Loop N is shown in Figure 7. The inserts are diagrammed in Figures 8 and 9.

One insert was an 8-in. section of 1-1/2-in. OD titanium 75A pipe machined to fit snugly inside the stainless steel piping and flanged in place so that the crevice between it and the stainless steel was dead-ended. The interior of the titanium pipe wall was tapered to give a smooth transition to the steel. The flow of solution through this insert was generally 40 gpm (about 7 fps) and was very turbulent since the pin and coupon holders were immediately upstream. In other loops, the stainless steel piping is frequently severely corroded in this region.

Examination of this flanged insert (Figure 8) showed there had been essentially no attack on the titanium. A large amount of loose scale was found in the crevice between the titanium and the stainless steel. This scale was magnetic and consisted largely of UO_2 and Fe_3O_4 indicating that oxygen exhaustion had occurred in the crevice. However, any accelerated attack on the stainless steel by the acid produced by oxygen exhaustion must have stifled itself since no significant decrease in wall thickness in the crevice region was apparent.

The other insert (Figure 9) was two straight sections of 1-1/2-in. OD titanium 75A pipe, one 12 in. and the other 3 in. long, machined to fit snugly inside the stainless steel pipe and rolled at the ends to prevent movement. They were butted end-to-end in a standard loop 15-in. stainless steel pipe section. The flow of solution through the insert was generally 10 gpm (about 2 fps) and also was very turbulent. Two 1/4-in. holes were drilled through the 12-in. insert opposite each other in order to facilitate removal of the insert. These holes exposed the stainless steel wall near the leading edge of the insert to solution.

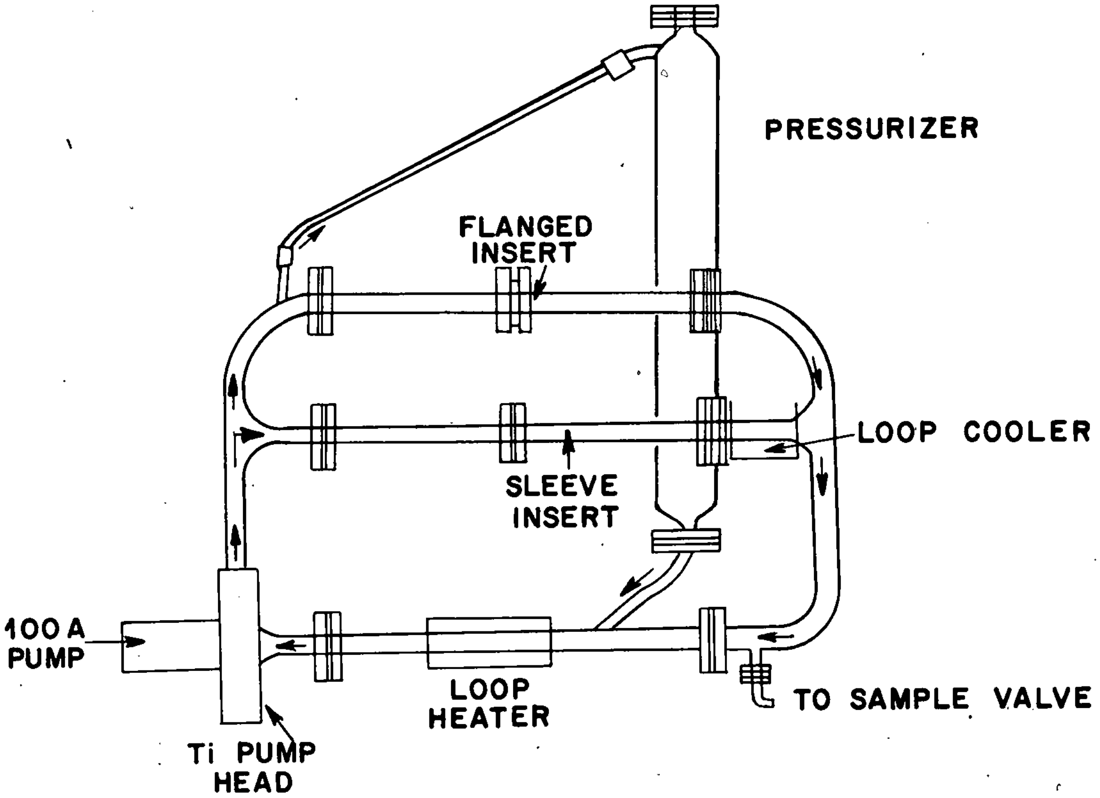

Fig. 7 Position of Titanium Inserts in Loop N

ORNL-LR-Dwg. -19445
UNCLASSIFIED

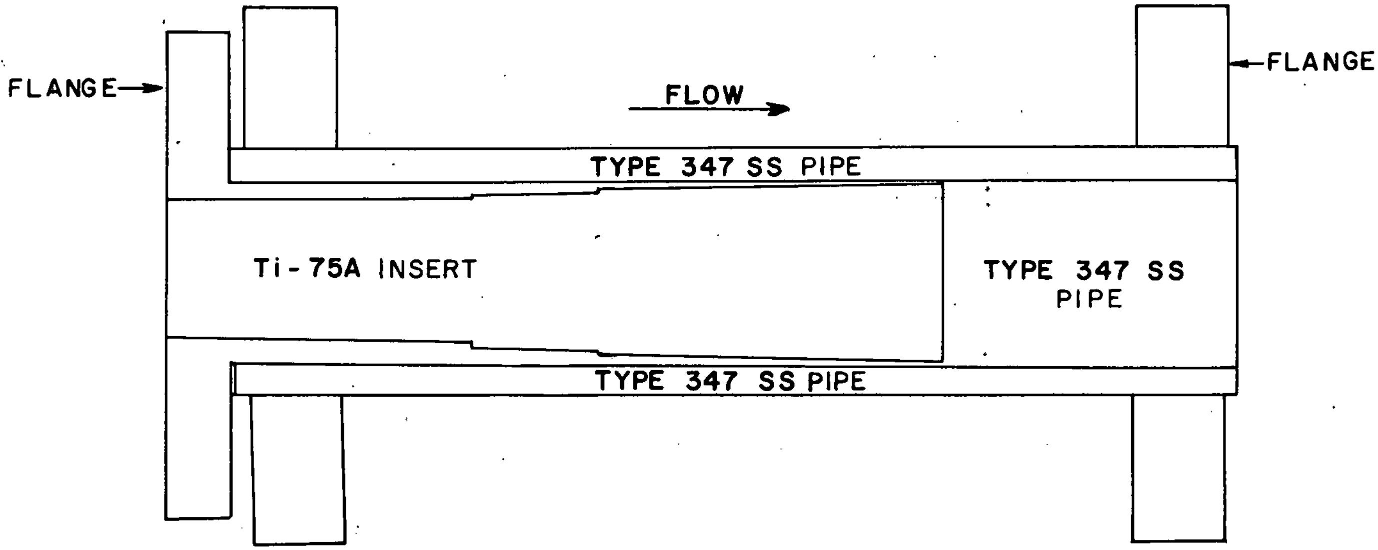

Fig. 8 Flanged Insert in Loop N
Runs N-1 through N-24
9901 hr

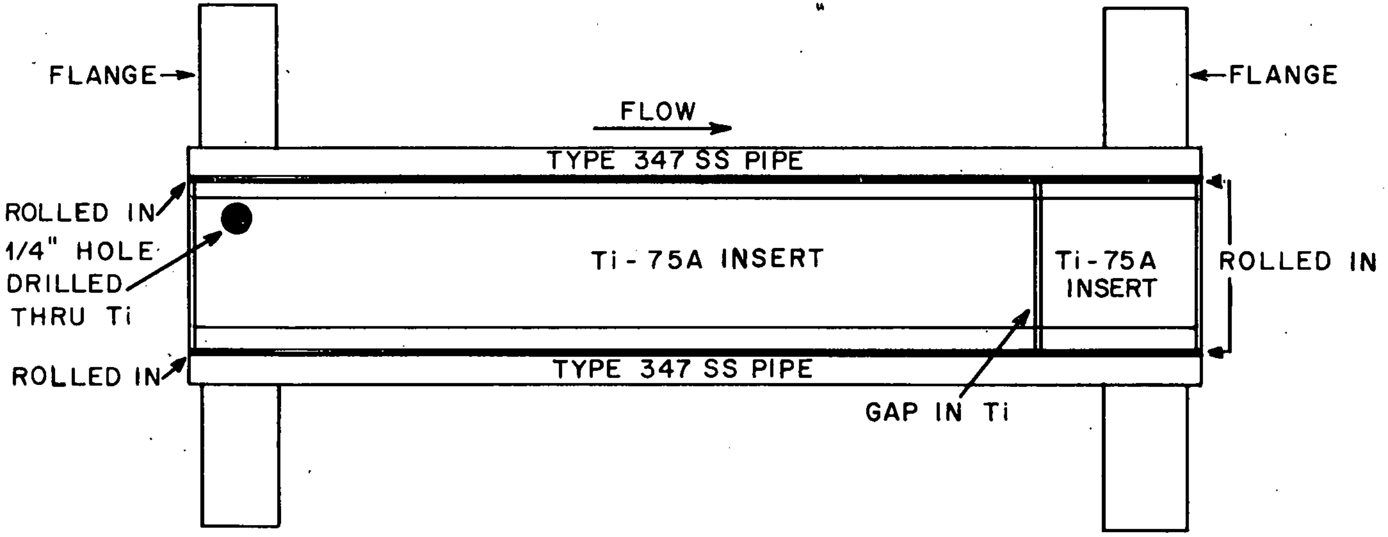

Fig. 9 Sleeve Insert in Loop N
Runs N-1 through N-24
9901 hr

Examination showed again no attack on the titanium. However, the stainless steel was corroded to a depth of about 1/16-in. where exposed at each 1/4-in. hole through the titanium. It appeared that the attack of the stainless steel was not due to a galvanic effect but rather to the fact that the flow of the uranyl sulfate solution was sufficiently turbulent to remove the protective coating from the stainless steel and allow the metal to corrode. Otherwise, the stainless steel under the titanium was covered with a thin film and had not been attacked, even where exposed at the thin gap between the 3-in. and 12-in. insert sections. A small amount of loose, non-magnetic scale was in the crevice between the titanium and the steel. Evidently, no oxygen exhaustion occurred in this crevice, perhaps because there was a significant flow of solution through the holes in the insert, along the crevice, and out where the inserts butted together.

It may be concluded that titanium liners in areas of high turbulence can protect the underlying steel piping and that the crevice formed need not lead to severe attack as was experienced previously(21). However, holes through the titanium, at least those as large as 1/4-in. in diameter, may not fill up with corrosion products and may lead to localized attack of the steel.

IV. LABORATORY CORROSION STUDIES (J. L. English, E. F. House, D. N. Hess, and J. C. Griess

A. Stress Corrosion of Type 347 Stainless Steel:

1. Effect of Halides in Uranyl Sulfate Solutions on Susceptibility to Cracking.

A laboratory-scale corrosion study to determine the susceptibility of stressed type 347 stainless steel to cracking in halide-containing boiling and aerated uranyl sulfate solutions was continued. The test medium was 0.04 m UO_2SO_4 solution containing 0.02 m H_2SO_4 and 0.005 m $CuSO_4$. The halide ion concentrations included in the study were 0, 5, 12, 25, 50, and 100 ppm of chloride and 100 ppm of bromide and iodide, respectively. The observations and results of the tests after 500 hr of exposure time have been reported in detail previously(22). Thus far, the tests have been operated for a total of 2000 hr.

More recently, the stress-cracking study was expanded to include chloride concentrations of 200 and 500 ppm and bromide concentrations of 50 and 200 ppm. The test conditions and the medium were the same as were used for the initial phase of the study. A total of 500 hr has been accumulated with these tests.

The corrosion-test specimens were three-point loaded, constant-strain assemblies of annealed type 347 stainless steel stressed at 15,000 and 30,000 psi. The stressed assemblies were exposed along with unstressed control specimens in the different test media. All specimens were removed after total elapsed exposure periods of 50, 100, 200, and 500 hr for examination for cracks and determination of corrosion rates. A complete summary of the corrosion data for the present and the preceding stress-cracking tests is included in Table VI.

It was reported that cracking occurred on the stressed type 347 stainless steel in uranyl sulfate solution containing 25 and 50 ppm of chloride, respectively, during the initial 100 to 200-hr exposure interval(22). In the present tests, suspected cracking was observed on stressed specimens in solutions containing 200 and 500 ppm of chloride ion at the end of 500 hr; the suspected cracks developed during the 200 to 500-hr exposure interval. Additional exposure time will be required to verify the existence of actual cracks. No cracks have been found on stressed specimens in solutions containing 0, 5, 10, or 100 ppm of chloride nor in solutions containing 50, 100, or 200 ppm of bromide or 100 ppm of iodide.

The attack on stressed and unstressed type 347 stainless steel by chloride-containing uranyl sulfate solution was predominantly generalized in nature with random pitting. The frequency and intensity of the pitting attack appeared more severe in solutions containing either 25 or 50 ppm of chloride ion. At chloride levels of 100 ppm and greater, the generalized attack increased in severity with increased chloride concentration; infrequent shallow pitting was observed also. At the lower chloride levels - 10 ppm and less - the attack was mildly-generalized with some random shallow pitting. Similarly, increasing the concentration of bromide ion from 50 to 100 and 200 ppm resulted in a more severe generalized corrosion attack on both stressed and unstressed specimens; shallow pitting was also evidenced. A few pits were observed on specimens in the uranyl sulfate solution containing 100 ppm of iodide; generalized attack was mild in the environment.

The effect of chloride ion in concentrations ranging from 0 to 500 ppm on the generalized corrosion attack of unstressed type 347 stainless steel by boiling and aerated 0.04 $\underline{m}$ UO_2SO_4 - 0.02 $\underline{m}$ H_2SO_4 - 0.005 $\underline{m}$ $CuSO_4$ solution is shown in Fig. 10. The observed weight losses on the stressed assemblies were not used to present the effect of chloride concentration because of a presently-unexplained lack of agreement with results for the unstressed control specimens. It was felt that the latter results would serve to present a more realistic view of the effect of chloride on the extent of corrosion attack. The weight loss data in Figure 10 were for duplicate unstressed control specimens exposed for a total of 500 hr in the respective test media. The 500-hr weight loss data for chloride concentrations from 0 to 100 ppm have been reported previously and indicated a leveling-off in the rate of attack with increased chloride concentration(22). However, the recent data with solutions containing 200 and 500 ppm of chloride showed the rate of corrosion attack to increase in linear fashion over the range of chloride concentrations from 50 to 500 ppm. The corrosion rates for both stressed and unstressed specimens of the type 347 stainless steel were found to decrease in magnitude with an increase in the total exposure time. The tests will be continued for an additional 1500 hr.

29

TABLE VI

Stress-Corrosion Behavior of Type 347 Stainless Steel in Boiling and Aerated 0.04 m UO_2SO_3 - 0.02 m H_2SO_4 - 0.004 m $CuSO_4$ Solution Containing Chloride, Bromide, and Iodide Additions

Test No.	Halide Conc. (ppm)	Stress Level (psi)	Total Time (hr)	Observed Corrosion Rate (mpy)	Observations
P-9	0	15,000	2000	<0.1	No cracks, uniform attack
		30,000	2000	<0.1	No cracks, uniform attack
P-10	5 Cl^-	15,000	2000	<0.1	No cracks, random pitting
		30,000	2000	<0.1	No cracks, random pitting
P-11	10 Cl^-	15,000	2000	0.6	No cracks, random pitting
		30,000	2000	0.2	No cracks, random pitting
P-12	25 Cl^-	15,000	1000(a)	1.5	Cracks formed during 200 to 500 hr interval, pitting attack
		30,000	1000(a)	5.6	Cracks formed during 100 to 200 hr interval, pitting attack
P-13	50 Cl^-	15,000	1000(a)	5.9	Cracks formed during 100 to 200 hr interval, pitting attack
		30,000	1000(a)	5.1	Cracks formed during 100 to 200 hr interval, pitting attack
P-14	100 Cl^-	15,000	2000	4.8	No cracks; random pitting
		30,000	2000	6.1	No cracks; random pitting
S-25	200 Cl^-	15,000	500	8.8	No cracks, random pitting
		30,000	500	12.4	Suspected cracks; pitting
S-26	500 Cl^-	15,000	500	9.8	Suspected cracks, random pitting
		30,000	500	13.5	Suspected cracks; random pitting
S-27	50 Br^-	15,000	500	<0.1	No cracks; random pitting
		30,000	500	<0.1	No cracks; random pitting
P-15	100 Br^-	15,000	2000	3.0	No cracks; random pitting
		30,000	2000	4.5	No cracks; random pitting
S-28	200 Br^-	15,000	500	1.6	No cracks; random pitting
		30,000	500	1.6	No cracks; random pitting
P-16	100 I^-(b)	15,000	2000	0.8	No cracks; random pitting
		30,000	2000	0.7	No cracks; random pitting

(a) Test terminated after 1000 hr.

(b) Concentration adjusted to approximately 100 ppm I^- at start of each run by addition of KI. Iodide content decreased during operation at boiling due to volatilization losses.

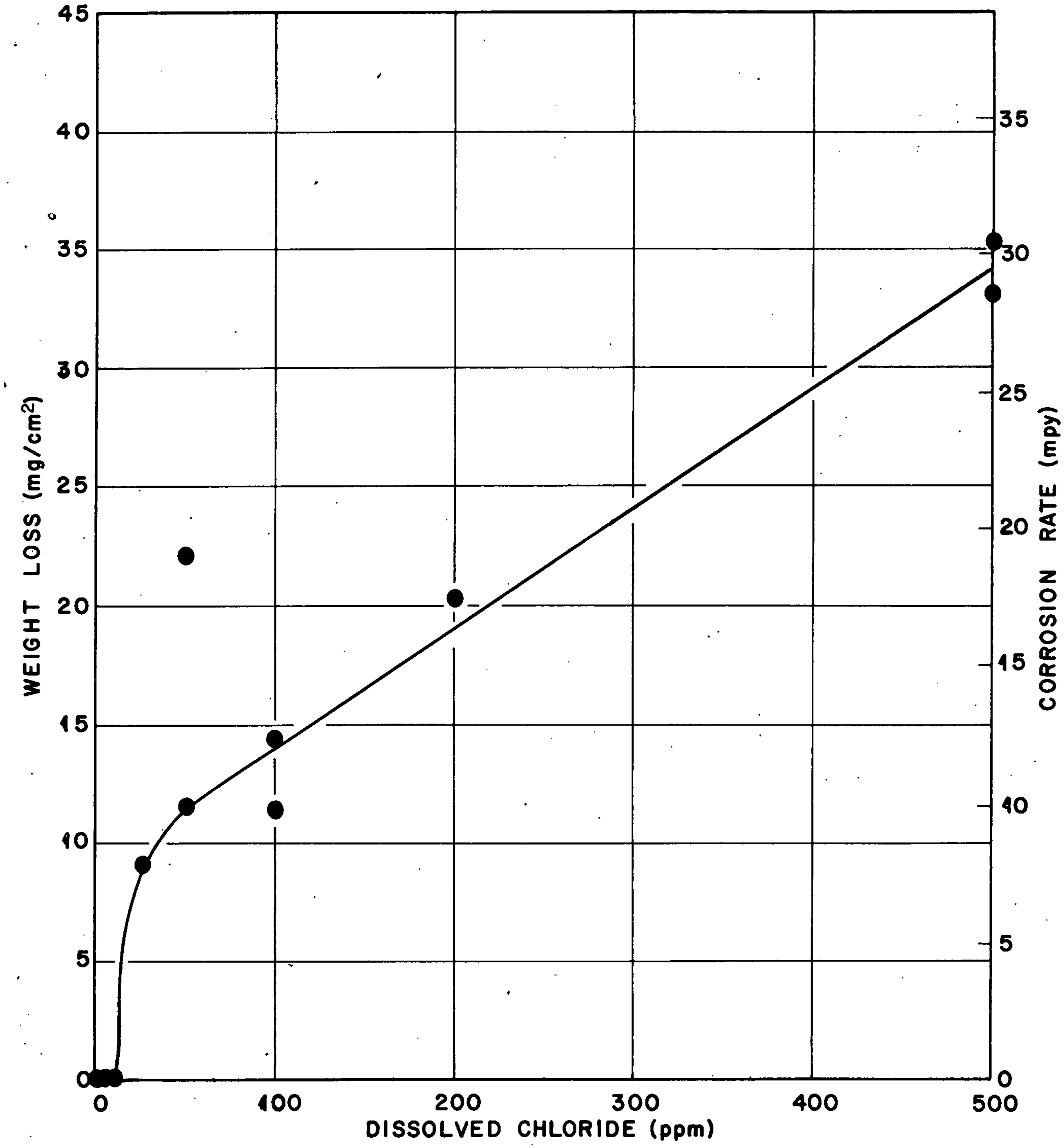

Fig. 10 The Effect of Chloride Ion Concentration on the Corrosion of Unstressed Type 347 Stainless Steel After 500 hr by Boiling and Aerated 0.04$\underline{m}$ UO_2SO_4 Solution Containing 0.02$\underline{m}$ H_2SO_4 and 0.005$\underline{m}$ $CuSO_4$

2. Inhibition of Stress-Corrosion Cracking.

A test program was initiated to examine possible remedial measures that might be considered for elimination of the susceptibility of the austenitic stainless steels, specifically type 347 stainless steel, to cracking in chloride-containing environments. One of the proposed protective measures that will be considered is the use of chemical corrosion inhibitors, including the pertechnetate ion, TcO_4^-. Also, the use of cathodic protection by means of sacrificial anodes will be investigated.

In order to evaluate the effectiveness of chemical additives on the suppression of cracking in austenitic type 347 stainless steel, it was necessary to establish the environmental test conditions such that consistently-reproducible cracking could be obtained. The major effort on the stress-cracking program during the past quarter was concerned with attempts to produce an environment that was capable of cracking stressed specimens of type 347 stainless steel with regularity. The results of this effort are described in the following section.

The environment that was found to produce consistent cracking within relatively-short periods of exposure was distilled water containing 100 ppm of chloride ion and various levels of dissolved oxygen at a temperature of 300°C. Approximately one-half of the chloride concentration in the distilled water was added as NaCl; the remaining half, as HCl which lowered the pH to a value of 2.8. Four concentration levels of dissolved oxygen were investigated: (1) normal oxygen which represented the available oxygen from air in the liquid and gas phases of the stainless steel autoclave at the start of the test; (2) 50 psi of oxygen (added initially as hydrogen peroxide) which corresponded to a dissolved oxygen content of approximately 450 ppm at the test temperature of 300°C; (3) 100 psi of oxygen (by tank oxygen gas addition to the autoclave at room temperature) which was estimated to be between 700 and 800 ppm of dissolved oxygen at 300°C; and (4) 150 psi of oxygen (by hydrogen peroxide addition) which corresponded to a dissolved oxygen content of approximately 1200 to 1300 ppm at 300°C.

Specimens of annealed type 347 stainless steel, 3/4 x 3 in. were cold-formed into a U-bend. The open ends of the "U" were drawn partially closed by means of a type 347 stainless steel tie-bolt to subject the specimen to a condition of elastically-applied stress. The U-bend specimens were placed in both solution and vapor phase of the test medium.

A summary of the results of the stress-corrosion cracking test appears in Table VII. In a total of 48 U-bend specimens that were exposed in the solution and the vapor phases of the chloride-containing distilled water at 300°C, cracks were observed on 40 of the specimens after exposure periods from 100 to 339 hr. The eight specimens that showed no indication of cracking were specimens that were exposed in the vapor above the test medium. Reproducibility of cracking in the solution phase was 100 per cent.

TABLE VII

Stress Cracking of Type 347 Stainless Steel at 300°C By Distilled Water Containing 100 ppm of Chloride

Test No.	Approximate O_2 Pressure (psi)	Total Hr	No. of Specimens	Specimens Location	Generalized Corrosion Rate (mpy)	Observations
U-21	Negligible(a)	199	1	Solution	0.5	Cracks
			1	Vapor	0.3	No Cracks
U-22	Negligible	199	1	Solution	0.8	Cracks
			1	Vapor	0.2	No Cracks
U-20	Negligible	339	1	Solution	4.9	Cracks
			1	Vapor	0.3	Cracks
U-23	Negligible	339	1	Solution	4.1	Cracks
			1	Vapor	1.6	Cracks
U-24	Negligible	339	1	Solution	4.1	Cracks
			1	Vapor	4.0	Cracks
U-17	50(b)	199	1	Solution	4.4	Cracks
			1	Vapor	0.3	No Cracks
U-18	50	199	1	Solution	2.9	Cracks
			1	Vapor	0.2	Cracks
U-15	50	339	1	Solution	7.4	Cracks
			1	Vapor	3.3	Cracks
U-16	50	339	1	Solution	4.3	Cracks
			1	Vapor	2.7	Cracks
U-19	50	339	1	Solution	7.7	Cracks
			1	Vapor	2.9	Cracks
U-29A	100(c)	140	4	Solution	14.5	Cracks
					12.9	Cracks
					16.7	Cracks
					14.9	Cracks
			4	Vapor	5.0	Cracks
					4.3	Cracks
					6.6	Cracks
					4.2	Cracks
U-29	100	199	4	Solution	5.8	Cracks
					4.4	Cracks
					5.4	Cracks
					5.9	Cracks
			4	Vapor	0.2	No Cracks
					0.2	No Cracks
					0.2	No Cracks
					0.2	No Cracks
U-29B	100	100	2	Solution (347 Stainless Steel Tie-bolts)	4.5	Cracks
					4.3	Cracks
			2	Solution (Carbon Steel Tie-bolts)	6.4	Cracks
					8.1	Cracks

TABLE VII (Continued)

Stress Cracking of Type 347 Stainless Steel at 300°C By Distilled Water Containing 100 ppm of Chloride

Test No.	Approximate O_2 Pressure (psi)	Total Hr	No. of Specimens	Specimens Location	Generalized Corrosion Rate (mpy)	Observations
U-17A	150(b)	140	1	Solution	8.5	Cracks
			1	Vapor	6.9	Cracks
U-17B	150	140	1	Solution	9.1	Cracks
			1	Vapor	0.2	No Cracks
U-18A	150	140	1	Solution	8.2	Cracks
			1	Vapor	9.4	Cracks
U-18B	150	140	1	Solution	9.3	Cracks
				Vapor	6.0	Cracks

(a) Oxygen content limited to the amount initially present from air in the gas and liquid phases of the test autoclave.

(b) Oxygen pressure produced by addition of 30% H_2O_2 to test medium.

(c) Autoclave pressurized with oxygen gas at room temperature at start of run.

The as-removed condition of the stressed specimens was characterized by heavy and non-uniform deposits of dark brown and black colored corrosion products. The solution-exposed specimens were more heavily-endowed with the deposits than the vapor-exposed specimens. The corrosion rates reported in Table VII were determined from observed weight losses after the specimens had been subjected to two successive 3-min cathodic defilming treatments in inhibited 5 wt % H_2SO_4 solution at 75°C using a current density of 20 amps/dm^2. The values for the generalized rates, although fairly high in most cases, were not necessarily indicative of the severity or extent of pitting attack. All of the specimens exhibited a marked tendency toward pitting; this tendency was more pronounced on solution-exposed than on vapor-exposed specimens.

One interesting phenomenom was presented by the stress-corrosion cracking behavior of the vapor-exposed specimens. Eight of the specimens exhibited no signs of cracking after exposure periods of 140 or 199 hr in the 300°C environment. In every case, the generalized corrosion rate for the specimens ranged from 0.2 to 0.3 mpy as compared with considerably-higher corrosion rates for the companion solution-exposed specimens which did exhibit cracking. With two exceptions - when cracks were found on vapor-exposed specimens - the generalized corrosion rates approached in magnitude the high values observed on the solution-exposed specimens. The two exceptions to this behavior occurred with specimens exposed in environments with negligible oxygen pressure and with approximately 50 psi of oxygen pressure (tests U-18 and U-20 in Table VII). The generalized corrosion rates for the two vapor-exposed specimens were similar to those experienced by specimens that did not show cracking, 0.2 and 0.3 mpy after 199 and 339 hr of exposure, respectively. However, both specimens were cracked. The corrosion rates for the solution-exposed companion specimens in the two tests were 2.9 mpy for the 199-hr test and 4.9 mpy for the 339-hr test.

It should also be emphasized from the data in Table VII that the incidence of cracking on the stressed specimens of type 347 stainless steel was independent of the dissolved oxygen content in the test medium. Cracking was observed on specimens in the chloride-containing distilled water with a low oxygen pressure as well as in water pressurized with an approximate oxygen pressure of 150 psi.

The use of cathodic protection to eliminate stress-corrosion cracking of type 347 stainless steel in boiling 42 wt % $MgCl_2$ solution by coupling the stainless steel with carbon steel has been reported by Compere(23). In the work by Compere, a specimen of the stainless steel stressed at 40,000 psi was placed in contact with carbon steel and exposed for 160 hr in boiling 42 wt % $MgCl_2$ solution at 154°C. Very active corrosion attack was experienced by the carbon steel, but no cracks developed on the type 347 stainless steel stress specimen during the 160 hr. Normally, uncoupled and stressed type 347 stainless steel evidenced cracking within several hours of exposure in the magnesium chloride environment.

In view of the above-reported behavior of stressed type 347 stainless steel coupled with carbon steel, it was decided to examine couples of the two materials in the present program with distilled water at 300°C containing 100 ppm of chloride. The specimens were the U-bend type as described previously. In place of the type 347 stainless steel tie-bolt used to draw the open ends of the "U" together, a carbon steel tie-bolt was substituted. Duplicate specimens of the couples along with duplicate specimens having type 347 stainless steel tie-bolts were placed in the solution phase of the water-chloride medium. The autoclave was pressurized with 100 psi of oxygen gas and heated at 300°C for 100 hr. The results of the test were not encouraging (test U-29B in Table II). Both specimens with the carbon steel tie-bolts underwent cracking during the 100-hr exposure as did the uncoupled type 347 stainless steel control stress specimens. The carbon steel tie-bolts showed excessive corrosion damage. It was concluded that in the particular environment under study, the coupling of stainless steel with carbon steel to eliminate cracking on the former was of no value. Further testing will be conducted to substantiate this conclusion, however. With an environment available that is capable of good reproducibility in stress-cracking type 347 stainless steel, work during the next quarter will be concentrated on the use of chemical corrosion inhibitors as a possible means of eliminating cracking. The initial effort will be concerned with the use of the pertechnetate ion for this purpose.

3. Stress-cracking of Type 347 Stainless Steel and Other Materials by Chloride-containing Cooling Water:

A 1000-hr run was completed on a pipe U-bend spray test operated under conditions that simulated those under which a service failure by cracking occurred in a dynamic-corrosion test loop(24). The construction and operational characteristics of the U-bend spray test have been reported previously(25). In resume, the test unit originally consisted of six U-bends of 3/8 and 1/2-in. sch 40 type 347 stainless steel pipe attached to common steam and condensate headers. Steam at 60 psig (153°C) was passed through the pipes which were externally-cooled by a continuous spray of Y-12 potable water containing an estimated dissolved chloride content of 3 to 7 ppm. Cracking was reported to have occurred on all six of the U-bends during nearly 11,000 hr of operation of the test and was attributed to the presence of approximately 760 ppm of chloride in the water-deposited scale that accumulated on the outer surfaces of the pipes(21).

The present 1000-hr run was made in a new spray-test unit that was constructed to accommodate 14 pipe U-bends. The operating conditions were the same as described in the preceding paragraph - internal heating with 60 psig steam and external cooling with chloride-containing filtered water. The investigation was concerned with the susceptibility of 1/2-in. sch 40 type 347 stainless steel pipe to stress-corrosion cracking by chloride-containing filtered cooling water as influenced by the initial heat-treated condition of the pipe. The heat treatments employed after cold forming the U-bend were annealing, sensitizing, and stress-relieving. Pertinent data for the various heat treatments are summarized in Table VIII. The effect of shot-peening on the cold-formed surfaces of a pipe U-bend to reduce susceptibility to cracking was examined also. A total of 12 pipe U-bends of type 347 stainless steel in the as-formed, sensitized, stress-relieved, annealed, and shot-peened conditions was exposed for the 1000-hr test in the cooling water spray test. Sensitized specimens of the type 347 stainless steel pipe were previously found acceptable by the boiling 65 wt % HNO_3 test; observed penetration rates (average for five 48-hr periods) were not in excess of an allowable value of 2.0 mils/month. In addition to the type 347 stainless steel U-bends, single U-bends of modified type 430 stainless steel (16 Cr - 1 Ni - 0.02 C) and MST Grade 3 titanium were placed in the spray test to determine the stress-corrosion cracking behavior of the two materials under the operating conditions of the spray test.

The incidence of cracking on the 14 pipe U-bends is summarized in Table VIII. Apparent cracking was found on all U-bends with three exceptions. Of the type 347 stainless steel U-bends, no cracking was observed after 1000 hr on the bends that were annealed for 1/2-hr at 1950°F before exposure nor on the single U-bend that was shot-peened after cold forming. Likewise, no cracks were found on the modified type 430 stainless steel U-bend. The MST Grade 3 titanium U-bend exhibited suspicious indications of cracking, but closer examination showed the suspected cracks to be scratches in the metal.

TABLE VIII

Stress-Corrosion Cracking of Steam-Heated Type 347 Stainless Steel and Other Materials Externally-Cooled for 1000 Hr by Chloride-Containing Potable Water

Material	Number of U-Bends	Initial Treatment	Observations
347SS	3	Cold-formed; no heat treatment; lightly pickled in HNO_3-HF	Numerous cracks on all 3 U-bends; many pits in crack areas
347SS	2	Cold-formed; sensitized 1 hr at 1250°F; air cooled; pickled in HNO_3-HF	Cracking frequency greater than on as-bent pipes; many deep pits associated with cracks and elsewhere
347SS	2	Cold-formed; heated 24 hr at 600°F; air cooled; pickled in HNO_3-HF	Numerous cracks on both specimens; many deep pits in crack areas
347SS	2	Cold-formed; heated 12 hr at 750°F; air cooled; pickled in HNO_3-HF	Less cracking than observed on 600°F-treated U-bends; many pits
347SS	2	Cold-formed; annealed 1/2 hr at 1950°F; water cooled; pickled in HNO_3-HF	No apparent cracks, many pits
347SS	1	Cold-formed; lightly grit-blasted; shot-peened	No apparent cracks, some pitting attack
430SS (mod.)*	1	Cold-formed; pickled in HNO_3-HF	No apparent cracks; some pitting attack
MST Gr 3 Ti	1	Cold-formed	No apparent cracks; random pitting

* Chemical composition: 16.1 Cr, 0.86 Ni, 0.02 C.

All pipes evidencing signs of cracking will be subjected to metallographic examination to verify the presence of cracks as indicated by the Super-Pentrex technique. The 14 U-bends were initially examined for the presence of cracks by the Super-Pentrex method after cold-forming and before subjecting to the various heat treatments; no cracks were found on any of the U-bends before their exposure to the chloride-containing cooling water.

In the majority of cases, the location of the cracks was on the tension side of the stressed pipe U-bends. No cracks were found on inner surfaces that were under compressive stress as the result of the cold forming operation. A considerable amount of pitting attack was present on all pipe U-bends. In instances where cracks were formed, the pits were intimately associated with the crack areas. Numerous cracks passed directly through pit sites, but there was no positive indication that cracking originated from a pit site.

Low-temperature stress-relieving heat treatments at 600 and 750°C were found to be ineffective in eliminating the susceptibility of the type 347 stainless steel pipe to cracking by the chloride-containing water; but in the latter case, the frequency of cracks appeared to be less than in the case of the 600°F stress-relieving treatment and considerably less than in the case of the U-bends sensitized at a temperature of 1250°F. Annealing at a temperature of 1950°F was successful in preventing cracking from occurring during the 1000-hr exposure. Shot-peening which placed the entire surface of the U-bend under compressive stresses was also successful for preventing the formation of cracks during the 1000-hr run.

The annealed and the shot-peened U-bends of type 347 stainless steel will be subjected to additional exposure in the spray test as will the U-bend pipe of modified type 430 stainless steel and other pipe bends of titanium alloys. Attention will be given to the use of cathodic protection for the prevention of stress-cracking of type 347 stainless steel such as might be obtained by contacting the stainless steel with aluminum during the exposure to the cooling water. Other factors affecting the susceptibility of type 347 stainless steel to stress-cracking will undergo examination. These factors will include different combinations of heating time and temperature in stress-relieving operations. An attempt will be made to determine if any correlation exists between the susceptibility of a material to cracking and its behavior in boiling 65% HNO_3.

B. Corrosion of Zirconium Alloys by Uranyl Sulfate Solution:

In cooperation with the HRP Metallurgy Group, a number of zirconium-base alloys has been tested in oxygenated uranyl sulfate solutions. In addition to supplying information on the general corrosion resistance of the various alloys, the test program was designed to furnish corrosion specimens for study of the oxide film structure by x-ray and by electron diffraction techniques. For the latter purpose, specimens were exposed for two periods, 100 hr and a maximum of 1000 hr. The 100-hr specimens will be used for electron diffraction examination of the films and the 1000-hr specimens will provide oxide for x-ray diffraction examination. The results of the film studies are not available at this time.

Corrosion data were obtained for alloys of zirconium with tantalum, molybdenum, niobium, and tin. Finger-type castings of the alloys were prepared by the HRP Metallurgy Group by arc melting in an inert atmosphere. After a homogenizing heat treatment for some of the alloys, the materials were cold rolled to a thickness of 0.1 or 0.06 in. and machined into corrosion-test specimens.

The specimens were exposed in oxygenated 0.04 m UO_2SO_4 solution containing 0.02 m H_2SO_4 and 0.005 m $CuSO_4$. The test temperature was 300°C. Two types of surface preparation were used on the specimens. In one case, the surfaces were mechanically-abraded on 180 grit paper; the other type of preparation was by chemical polishing in a nitric-sulfuric-hydrofluoric acid solution. The specimens were insulated from the stainless steel test containers with Teflon hangers during the high-temperature exposure.

The observed corrosion rates included in Table IX were determined from the as-removed and scrubbed weight losses on the specimens. A considerable number of the specimens exhibited weight gains rather than weight losses after an 804 or 1000-hr exposure in the uranyl sulfate solution.

The least corrosion-resistant alloy tested was the 10Mo-90Zr alloy which corroded at rates of 3.6 and 4.5 mpy for duplicate specimens after 804 hr; the surfaces of the specimens were initially prepared by chemical polishing. Other alloys that showed corrosion rates included a chemically-polished specimen of the 5Mo-10Nb-85Zr alloy which was corroded at a rate of 1.5 mpy in 1000 hr and chemically-polished specimens of the 5Mo-15Nb-80Zr and 5Mo-10Nb-5Ta-80Zr alloys that were corroded at a rate of 0.9 mpy in 1000 hr. A corrosion rate of 0.2 mpy was observed on a mechanically-polished specimen of the 5Mo-10Nb-85Zr alloy after an exposure period of 804 hr.

The behavior of mechanically-polished and chemically-polished specimens of the remaining alloys which included 33Nb-67Zr, 7Mo-20Nb-73Zr, and 3Sn-15Nb-82Zr compositions was characterized by weight gains ranging from 0.1 to 0.8 mg/cm^2. By comparison with the corrosion behavior of the present alloy series undergoing test, cast specimens of Zircaloy-2 exposed in a somewhat similar environment at 300°C showed a negligible weight change after 1000 hr. The environment for the Zircaloy-2 test was oxygenated 0.04 m UO_2SO_4 solution containing 0.004 m H_2SO_4 and 0.005 m $CuSO_4$.

Three of the six alloys that were supplied with both mechanically- and chemically-polished specimens showed an appreciable difference in corrosion behavior between the two types of initial surface preparation. The three alloys showing this difference in behavior were of the following compositions: 5Mo-10Nb-85Zr, 5Mo-15Nb-80Zr, and 5Mo-10Nb-5Ta-80Zr. The mechanically-polished specimens of the alloys exhibited slight weight gains - not in excess of 0.3 mg/cm^2 - or near-negligible corrosion rates after 804 hr in the oxygenated uranyl sulfate solution at 300°C whereas the chemically-polished specimens of similar alloy type showed corrosion rates after 1000 hr of 0.9 or 1.5 mpy. In all cases, attack on specimens with both types of surface preparation was uniform. Similarly, uniform attack was observed on mechanically- and chemically-polished specimens of the other zirconium-base alloys included in the investigation.

TABLE IX

The Corrosion of Zirconium-Base Alloys by Oxygenated 0.04 m UO_2SO_4 - 0.02 m H_2SO_4 - 0.005 m $CuSO_4$ Solution at 300°C

Test No.	Material Identity	Alloy Composition (w/o)	Heat Treatment	Specimen Condition	Total Hr	Observed Weight Change (mg/cm^2)	Specimen Condition
S-74	Zr-42	33Nb-67Zr	No heat treatment; cold-rolled directly from casting to 0.06-in. thick	Mechanically-polished	804	(1) + 0.3 (2) + 0.1	Dull medium-dark gray uniform film; uniform attack
S-16	Zr-42	33Nb-67Zr	Same as above	Chemically polished	1000	+ 0.5	Lustrous brown-and-gray thin film; uniform attack
S-78	Zr-18	10Mo-90Zr	Hot-rolled at 700°C to 0.1 in.; cold-rolled to 0.06 in.	Chemically polished	804	(1) - 5.8 (2) - 7.4	Mottled green-and-brown film; surfaces heavily roughened; uniform attack.
S-71	Zr-12	5Mo-10Nb-85Zr	Homogenized 7 hr at 1175°C; water quenched; cold-rolled to 0.1 in.	Mechanically-polished	804	(1) - 0.2 (2) negligible	Dull yellow-and-brown streaked film; uniform attack
S-13	Zr-12	5Mo-10Nb-85Zr	Same as above	Chemically polished	1000	- 3.0	Mottled gray-and-green film, uniform attack
S-73	Zr-17	5Mo-15Nb-80Zr	Homogenized 2 hr at 1175°C; water quenched; cold-rolled to 0.1 in.	Mechanical-polished	804	+ 0.3	Semi-lustrous dark brown-and-black film; uniform attack
S-15	Zr-17	5Mo-15Nb-80Zr	Same as above	Chemically-polished	1000	- 1.9	Mottled gray-and-black film; uniform attack
S-81	Zr-47	7Mo-20Nb-73Zr	No heat treatment; cold-rolled directly from casting to 0.1 in.	Chemically-polished	804	+ 0.1	Lustrous dark gray film with yellow streaks, uniform attack

TABLE IX .(Continued)

The Corrosion of Zirconium-Base Alloys by Oxygenated 0.04 $\underline{m}$ UO_2SO_4 - 0.02 $\underline{m}$ H_2SO_4 - 0.005 $\underline{m}$ $CuSO_4$ Solution at 300°C

Test No.	Material Identity	Alloy Composition (w/o)	Heat Treatment	Specimen Condition	Total Hr	Observed Weight Change (mg/cm^2)	Specimen Condition
S-72	Zr-14	5Mo-10Nb-5Ta-80Zr	Homogenized 7 hr at 1175°C; water quenched; cold-rolled to 0.1 in.	Mechanically-polished	804	+ 0.2	Dull dark brown-and-black film; uniform attack
S-14	Zr-14	5Mo-10Nb-5Ta-80Zr	Same as above	Chemically polished	1000	- 1.9	Mottled dark gray-and-black film; uniform attack
S-75	Zr-67	3Sn-15Nb-82Zr	No heat treatment; cold-rolled directly from casting to 0.06 in.	Mechanically polished	804	(1) + 0.4 (2) + 0.5	Dark gray film with white streaks; uniform attack
S-17	Zr-67	3Sn-15Nb-82Zr	Same as above	Chemically-polished	1000	+ 0.8	Mottled gray-and-black film; uniform attack

Future work will be concerned with a study on the effect of additions of iron, palladium, nickel, tin, vanadium, and yttrium on the corrosion behavior of zirconium-niobium base alloys in oxygenated uranyl sulfate solution at 300°C. The corrosion behavior of binary alloys of zirconium with palladium, manganese, titanium, indium, uranium, platinum, chromium, and silicon will also be investigated.

C. Corrosion of Elgiloy by Uranyl Sulfate Solution:

The behavior of Elgiloy - a spring material considered for use in the HRT liquid-level controller with a nominal chemical composition in weight per cent of 20Cr-15Ni-2Mn-7Mo-40Co - in oxygenated uranyl sulfate solution at 300°C has been described previously(27). Although the alloy was found to possess satisfactory corrosion resistance in both solution and vapor phases of the 0.04 $\underline{m}$ UO_2SO_4 solution containing 0.02 $\underline{m}$ H_2SO_4 and 0.005 $\underline{m}$ $CuSO_4$, later tests showed the alloy to be susceptible to stress-corrosion cracking in a similar environment known to contain less than 2 ppm of dissolved chloride ion(28). Corrosion studies with Elgiloy during the past quarter were concerned with the use of various pickling and heat treatments to minimize or preferably eliminate the susceptibility of the alloy to stress-corrosion cracking in oxygenated uranyl sulfate solution at elevated temperature. The Elgiloy used for the corrosion tests was received as 0.030 in. thick strip which was cold-rolled to 85% reduction in area. The as-received hardness of the strip was between 50 and 51 Rockwell C; the yield strength was reported as 150,000 to 170,000 psi.

Two approaches were used in an attempt to eliminate the stress-cracking susceptibility of the alloy. One approach dealt with the use of pickling or electropolishing treatments on the test specimens to remove residual surface stresses which may have been produced during cold-rolling of the strip. The second approach was concerned with the use of an annealing treatment at 2100°F to remove all surface and internal stresses in the alloy strip.

The general corrosion resistance and the resistance to stress-cracking of hardened Elgiloy strip was examined, also. The hardened specimens were pickled or electropolished prior to test. The hardness of the alloy after heat treatment for 5 hr at 900°F was increased from the as-received hardness of 50 to 51 Rockwell C to a value of 56 Rockwell C.

The environment for the stress-corrosion cracking tests was oxygenated 0.04 $\underline{m}$ UO_2SO_4 solution containing 0.02 $\underline{m}$ H_2SO_4 and 0.005 $\underline{m}$ $CuSO_4$ at a temperature of 300°C. Hydrogen peroxide additions were used to supply the desired oxygen pressure of approximately 150 psi at the test temperature.

The Elgiloy specimens were carefully prepared from the 0.030-in. thick strip for solution and vapor exposure in the uranyl sulfate solution. Vapor-phase specimens were included in the investigation since in actual HRT operation, the liquid-level control springs operate in the vapor phase above the uranyl sulfate fuel solution. The specimens were identified with the aid of a Vibra-tool, rather than by stamping, in order to minimize the possibility of cracking occurring at stamped identification numbers.

TABLE X

Corrosion Behavior of Elgiloy in Oxygenated Distilled Water and in Oxygenated Uranyl Sulfate Solution at 300°C

Test No.	Specimen Medium	Specimen Treatment	Specimen Location	Total Hr	Observed Corrosion Rate (mpy)	Specimen Condition
R-18	Distilled H_2O	As-received(1)	Solution	1524	0.1	Mottled thin film; no cracks
			Vapor	1524	Gain	Mottled thin film; no cracks
R-12	0.04 m UO_2SO_4 0.02 m H_2SO_4 0.005 m $CuSO_4$	As-received	Solution	2000	1.7	Uniform attack; cracks on edges
			Vapor	2000	0.3	Uniform attack; cracks on edges
R-13	Same as above	As-received; pickled in HNO_3-HF	Solution	2000	2.3	Uniform attack; cracks and splitting along edges; less severe on vapor-exposed specimen
			Vapor	2000	0.4	
R-17	Same as above	As-received; electropolished in H_3PO_4-CrO_3	Solution	1524	2.4	Uniform attack with cracks and splitting along edges; less severe on vapor-exposed specimen
			Vapor	1524	2.0	
R-14	Same as above	Annealed 20 min at 2100°F; air cooled; pickled in HNO_3-HF(2)	Solution	1524	4.9	Uniform attack; no cracking
			Vapor	1524	1.0	Uniform attack; no cracking
R-15	Same as above	Hardened 5 hr in air at 900°F; air cooled; pickled in HNO_3-HF(3)	Solution	1524	2.2	Uniform attack with cracks and splitting along edges
			Vapor	1524	1.3	
R-16	Same as above	Hardened 5 hr in air at 900°F; air cooled; pickled; electropolished in H_3PO_4-CrO_3	Solution	1524	2.3	Uniform attack; no cracks observed on either specimen
			Vapor	1524	2.2	

(1) As-received hardness, 50 to 51 Rockwell C.
(2) Hardness after annealing, 85 Rockwell B.
(3) Hardness after heat treatment, 56 Rockwell C.

Results of the corrosion tests are summarized in Table X. A test was run in oxygenated distilled water at 300°C with the as-received material to serve as a control for comparing with the stress-corrosion cracking behavior of the alloy in uranyl sulfate solution. No cracking was observed on the solution- or vapor-exposed specimens after 1524 hr in the distilled water environment.

In uranyl sulfate solution at 300°C, cracks were found on as-received and pickled specimens, as-received and electropolished specimens, and on hardened and pickled specimens at the completion of 1524 and 2000-hr exposure periods. The appearance of cracks which were present on both solution and vapor phase specimens was noted considerably earlier in the tests. The cracks were located for the most part at the edge surfaces. In addition to cracks, the specimens showed splitting of the metal along edge surfaces. The intensity of the splitting action was more severe on the solution-exposed specimens than on the vapor-exposed specimens.

No cracks were found on solution- and vapor-exposed specimens of as-received Elgiloy during 1524 hr in distilled water at 300°C nor on solution- and vapor-exposed specimens of annealed Elgiloy during 1524 hr at 300°C in the uranyl sulfate solution. Corrosion attack on the alloy by both environments was uniform. The intensity of the attack by the solution phase in the distilled water was very mild, 0.1 mpy; the vapor-exposed specimen exhibited a slight weight gain. Corrosion rates for the uranyl sulfate solution were considerably higher - 4.9 mpy in the solution and 1.0 mpy in the vapor. It was of interest to note that the corrosion resistance of annealed Elgiloy was only one-half as good as the corrosion resistance of the hardened Elgiloy in the solution phase of the uranyl sulfate. This observed behavior was in agreement with published information comparing the general corrosion resistance of annealed and hardened Elgiloy(29).

Further corrosion studies with Elgiloy will be dependent upon whether or not the alloy may be successfully used as a spring material in the annealed condition. In this condition, tests to date have indicated that the alloy is not subject to stress-corrosion cracking by uranyl sulfate solution at elevated temperature.

D. Corrosion of Various Materials by 4 M Sulfuric Acid Solution:

Corrosion tests have been continued with a number of materials of possible interest for the HRT chemical processing plant in 4 $\underline{M}$ H_2SO_4 with and without the addition of simulated fission and corrosion products(30). With the decision to use stabilized Carpenter 20 stainless steel for fabrication of a number of components such as tanks, pumps, valves, etc. for the chemical processing plant, most of the corrosion studies during the past quarter have been concerned with an examination of the corrosion behavior of Carpenter 20-Cb specimens cut from the materials being used in the actual fabrication of the above components. The environment selected for the testing of Carpenter-20 was boiling and oxygenated 4 $\underline{M}$ H_2SO_4 solution containing simulated fission and corrosion product additions. In the next few paragraphs, the results obtained with Carpenter-20 stainless steel representative of the material used in the HRT chemical processing plant will be discussed.

Duplicate specimens from 2-1/4 and 3-1/4-in. square bars of Carpenter 20-Cb stainless steel were used. Single specimens of Carpenter 20-Cb pipe and pipe welded to type 347 stainless steel with Carpenter 20-Cb weld rod were exposed also. The average corrosion rates are reported in Table XI. The corrosion rates were determined from the weight loss on the duplicate specimens during the entire period of the test. All of the specimens with the exception of the two pipe sections were prepared for test by polishing with 80 and 120 grit papers. Only the ends of the pipe section were given similar treatment. The specimens were immersed in acetone and in alcohol, dried, and weighed.

The data reported in Table XI are for boiling and oxygenated 4 $\underline{M}$ H_2SO_4 solution to which the following salts were added: $Zr(SO_4)_2$, 56 g/l; $Fe_2(SO_4)_3$, 75 g/l; $Cr_2(SO_4)_3$, 24 g/l; $Ru(SO_4)_2$, 0.4 g/l; UO_2SO_4, 28 g/l; and $CuSO_4$, 1.5 g/l. The specimen identification was supplied by the Chemical Technology Division.

TABLE XI

Corrosion of Carpenter 20-Cb Stainless Steel
in 4 $\underline{M}$ H_2SO_4 Solution Containing Simulated
Fission and Corrosion Products

Temperature - Boiling (111°C) Atmos - Oxygen

Specimen Identification	Original Material Description	Total Hr	Corrosion Rate (mpy)
B	2 1/4-in. square bar	214	7.5
O	3 1/4-in. square bar	214	3.2
Ⓑ	3 1/4-in. square bar	214	3.3
P	2 1/4-in. square bar	214	3.1
M	2 1/4-in. square bar	214	2.8
Welded joint of Carpenter 20-Cb and type 347 SS		266	20.4

All of the specimens with the exception of the welded pipe joint and the specimen B (machined from 2 1/4-in. square bar) showed a uniform corrosion attack. The surfaces of the specimens were covered with a thin, blue-white colored film. No cracks were noted at locally-stressed areas such as stamped identification numbers, sharp corners, etc. The observed corrosion rates were either decreasing slightly or remaining constant with time.

The welded pipe joint was 3/4-in. sch 40 Carpenter 20-Cb stainless steel pipe welded with Carpenter 20-Cb rod to type 347 stainless steel pipe of comparable size. The circumferential weld metal exhibited crater corrosion attack at several sites. The longitudinal weld in the Carpenter 20-Cb pipe showed a prominent knife-line attack in the base metal immediately adjacent to the weld. The weld metal also exhibited a narrow band of highly-localized corrosion attack extending along the center of the weld. The observed corrosion rate, 20.4 mpy for 266 hr, was decreasing with increased exposure time.

One of the duplicate specimens identified as B had two deep pits on one flat surface and cracks across an edge surface. The network of cracks also extended onto the flat surface of the specimen. Neither pitting nor cracking was observed on any of the other Carpenter 20-Cb stainless steel specimens.

In a previous report, the corrosion resistance of a number of materials in boiling 4 M H_2SO_4 free of oxygen and fission and corrosion products was reported(30). During the past quarter, the same materials were exposed to boiling 4 M H_2SO_4 free of added fission and corrosion products but through which oxygen was passed during the test. The results of the test are presented in Table XII; the results obtained in the absence of oxygen are presented for comparison.

Graphitar-14, Zircaloy-2, zirconium, and tantalum showed negligible corrosion rates in both systems. Sintered aluminum oxide appeared to demonstrate a higher corrosion rate in the absence of oxygen, but it is not certain that this is a real difference. Aluminum oxide is somewhat porous, and it is frequently difficult to dry the material to a constant weight. Stellites 98M2 and 6 showed considerably lower corrosion rates in the absence of oxygen than in its presence but in both cases, the corrosion rates were high. Lead, Illium-R and Hastelloy B showed uniform corrosion both in the presence and absence of oxygen but the lower corrosion rates were observed in the reducing environment; the same was true for types 316 and 347 stainless steel although the corrosion rates were extremely high in both systems. On the other hand, Carpenter 20-Cb showed a lower generalized corrosion rate in the presence of oxygen than in its absence; in both environments, stress-corrosion cracking was observed in locally stressed areas. The pipe specimen of Carpenter 20-Cb stainless steel in Table XII was sectioned from a 90° 1/2-in. sch 40 elbow. Cracks and pits appeared in the inner and outer radii of the bend and also on the inner surface of the longitudinal weld in the pipe.

Further testing is in progress with some of the materials listed in Table XII in 4 M H_2SO_4 at 100°F where corrosion should be much less severe. In addition, new tests with Carpenter 20-Cb stainless steel specimens representing materials used in the fabrication of the HRT chemical process plant components will be started in the boiling acid solution to which simulated fission and corrosion products have been added. As it was pointed out in a previous report(30), the presence of the fission and corrosion products in the sulfuric acid solution greatly reduces the general corrosion rates of Carpenter 20-Cb and type 347 stainless steel and the susceptibility of Carpenter 20-Cb to stress-corrosion cracking. Tests will be carried out to determine the effect of applied stress on the cracking of both Carpenter 20-Cb and type 347 stainless steel in the acid solution containing the added salts.

TABLE XII

Corrosion of Various Materials by Boiling 4 M H_2SO_4 Solution at 190°C

Material	Oxygen Atmosphere		Helium Atmosphere	
	Total Hr	Corrosion Rate (mpy)	Total Hr	Corrosion Rate (mpy)
Aluminum oxide	335	2.3	547	10.0
Carpenter 20-Cb	335	13.0	524	32.0
Carpenter 20-Cb (Pipe Bend)	311	11.0	-	-
Graphitar-14	335	Gain	530	Gain'
Hastelloy-B	335	22.0	437	33.2
Illium-R	335	38.0	437	15.0
Lead	335	8.0	436	1.0
Stellite 98M2	101	2450	40	150
Stellite 6	3.5	28,000	2.5	1100
Tantalum	335	< 0.1	442	0
347 SS	3.5	117,000	4.5	2500
316 SS	3.5	79,000	4.5	2000
Zircaloy-2	335	0.1	437	0
Zirconium	335	0.1	437	0

V. REFERENCES

1. H. C. Savage, J. C. Griess, et al., Quarterly Report of the Solution Corrosion Groups for the Period Ending Oct. 31, 1956, ORNL CF 56-10-13, pp 5-9.

2. T. H. Mauney, R. S. Greeley, et al., Operating Test of HRT Core Vessel Transition Joint and Expansion Bellows Mockup, ORNL CF 57-1-68.

3. Reference 1, p 7.

4. Ibid., p 6.

5. The bellows is of two ply construction. Each ply is 0.050 in. thick type 347 stainless steel.

6. Reference 1, p 11.

7. R. S. Greeley, et al., HRP Dynamic Corrosion Studies: Summary of Run K-17. 0.04 m UO_2SO_4 + 0.02 m H_2SO_4 + 0.005 m $CuSO_4$ at 300°C. November 23, 1956. ORNL CF 56-11-104, p 2.

8. Reference 1, p 12.

9. J. C. Griess, et al., HRP Dynamic Corrosion Studies: Quarter Ending July 31, 1956, ORNL CF 56-7-52, p 29.

10. Idem.

11. Reference 1, p 7 and 10.

12. J. C. Griess, et al., Quarterly Report of the Solution Corrosion Group for the Quarter Ending April 30, 1956, ORNL CF 56-4-138, p 29.

13. Reference 1, p 15.

14. Reference 9, pp 18-24.

15. J. C. Griess, HRP Quar. Prog. Rep., July 31, 1954, ORNL-1772, p 75.

16. J. C. Griess and R. S. Greeley, HRP Quar. Prog. Rep., April 30, 1955, ORNL-1895, pp 83-87.

17. J. L. English and E. L. Compere, HRP Quar. Prog. Rep., Jan. 31, 1955, ORNL-1853, p 121.

18. J. C. Griess and H. C. Savage, HRP Quar. Prog. Rep., April 30, 1954, ORNL-1772, p 76.

19. Reference 9, p 9.

20. H. C. Savage and F. J. Walter, HRP Quar. Prog. Rep., April 30, 1954, ORNL-1772, p 59.

21. Ibid., p 61.

22. J. L. English and J. C. Griess, HRP Dynamic Corrosion Studies, ORNL-CF 56-7-52, July 31, 1956, pp 36-43.

23. E. L. Compere, HRP Quar. Prog. Rep for Period Ending July 31, 1955, ORNL-1943, p 133.

24. H. C. Savage and F. J. Walter, HRP Quar. Prog. Rep. Ending April 30, 1954, ORNL-1753, p 59-61.

25. E. L. Compere and J. L. English, HRP Quar. Prog. Rep. Ending July 31, 1954, ORNL-1772, p 94.

26. J. L. English and J. C. Griess, Quar. Rep. of the Solution Corrosion Group Ending April 39, 1956, ORNL CF 56-4-138, p 31-36.

27. J. L. English and J. C. Griess, HRP Quar. Prog. Rep. Ending January 31, 1956, ORNL-2057, p 86.

28. J. L. English and J. C. Griess, Quar. Rep. of the Solution Corrosion Group Ending April 30, 1956, ORNL CF 56-4-138, p 32.

29. Kenneth Rose, Highly Corrosion Resistant Spring Material Finds Varied Use, Materials and Methods, September, 1950.

30. J. L. English, et al., Quar. Rep. of the Solution Corrosion Group Ending October 31, 1956, ORNL CF 56-10-13, pp 18-23.

1-48